

COST OPTIMISATION OF GLUED LAMINATED TIMBER ROOF STRUCTURES USING GENETIC ALGORITHMS

J. R. Villar-García¹, P. Vidal-López², D. Rodríguez-Robles³, M. Guaita⁴

1: Department of Forest and Agricultural Engineering, University Center of Plasencia, University of Extremadura, Av. Virgen del Puerto 2, 10600 Plasencia, Spain. e-mail: jrvillar@unex.es **Corresponding Author**

2: Department of Forest and Agricultural Engineering, Faculty of Agricultural Engineering, University of Extremadura, Av. Adolfo Suarez s/n, 06071 Badajoz, Spain. e-mail: pvidal@unex.es

3: Department of Forest and Agricultural Engineering, Faculty of Agricultural Engineering, University of Extremadura, Av. Adolfo Suarez s/n, 06071 Badajoz, Spain. e-mail: desireerodriguez@unex.es

4: Structural Timber Engineering Platform PEMADE, Department of Agroforest Engineering, University of Santiago de Compostela, Higher Technical School, C/Benigno Ledo s/n, 27002 Lugo, Spain. e-mail: m.guaita@usc.es

Abstract

Roof structures comprising of heavy timber trusses and purlins made of glued laminated timber, as well as dowels and metal plates used as mechanical joints, are widely employed, among others, in agro-industrial settings that require large open areas. This paper presents the economic optimisation of such roof structures through the use genetic algorithm models. Two phases of optimisation were carried out: firstly, in two dimensions for a single truss and, then, an entire roof structure in three dimensions. Both models followed a discrete approach, i.e. the optimisation of the cross-section was limited by the characteristics of the commercially-available glulam timber boards, an aspect not yet included in the literature. Therefore, the models allowed the influence of the laminate thickness in the optimisation to be estimated, but also allow comparisons with the continuous cross-section variation found in the literature. Furthermore, the optimisation took into account a range of configurations of trusses, number of joints and separation between trusses and purlins. The genetic algorithms were shown as an efficient optimisation tool for roof glulam structures as a function of the laminate thickness. Among the results obtained, the most cost-effective solutions were those comprised of the fewer number of joints in the trusses and the lowest laminate thickness of those studied. Moreover, the optimal separations between trusses and purlins were also determined. Finally, a simplified method of optimum pre-dimensioning was also proposed.

Keywords: Roof Structures; Timber Trusses; Glulam Timber; Genetic Algorithms; Structural Optimisation.

Symbols

a_1	Spacing, parallel to grain, of fasteners within one row [mm]
a_2	Spacing, perpendicular to grain, between rows of fasteners [mm]
$a_{3,c}$	Distance between fastener and unloaded end [mm]
$a_{3,t}$	Distance between fastener and loaded end [mm]
$a_{4,c}$	Distance between fastener and unloaded edge [mm]
$a_{4,t}$	Distance between fastener and loaded edge [mm]

43	A_i	Cross-section of member i [mm ²]
44	A_i^*	Effective cross-section of member i [mm ²]
45	b	Width of a cross-section [mm]
46	$ct_{dowel+steel}$	Materials and labour costs per fastener for handling, assembling, drilling, and
47		bolting, including the adjoining steel plates [€ dowel ⁻¹]
48	ct_{GL}	Price of the manufactured and embedded timber per m ³ [€ m ⁻³]
49	ct_{hanger}	Materials and manual labour costs for handling and assembling one purlin hanger,
50		3.75 [€ hanger ⁻¹];
51	$c_e(z)$	Wind exposure factor
52	d	Fastener diameter [mm]
53	E_{mean}	Mean value of the elastic modulus [N mm ⁻²]
54	$E_{0.05}$	Fifth percentile of the elastic modulus [N mm ⁻²]
55	$F(x)$	Modified objective function [€]
56	$f(x)$	Objective function [€]
57	$G_j(x)$	Maximum ultimate limit state utilisation ratio in each bar j
58	h	Height of a cross-section [mm]
59	ht	Edge depth (i.e. height at the truss supports) [m]
60	Ht	Greatest depth of the truss (i.e. midpoint height) [m]
61	j	Number of variables studied
62	k_{mod}	Modification factor, which takes into account the effect of the duration of the load
63		and the moisture content
64	K_{ser}	Slip modulus
65	K_u	Instantaneous slip modulus for ultimate limit states
66	L	Span of the truss [m]
67	l_i	Length of member i [mm]
68	n	Number of members of the upper chord
69	$n_{a,i}, n_{e,i}$	Number of fasteners at the beginning and end of member i
70	n_{lam}	Number of laminates in a cross-section
71	N_{dowels}	Total number of dowels in a truss
72	$N_{trusses}$	Total number of trusses for a "roof individual"
73	$N_{purlins}$	Total number of purlins for a "roof individual"
74	$P_j(G_j(x))$	Penalisation of the objective function in accordance with the ultimate limit state [€]
75	q_b	Wind basic velocity pressure
76	$S(x)$	Maximum ultimate limit state utilisation ratio
77	$T(S(x))$	Penalisation of the objective function in accordance with the serviceability limit
78		state [€]
79	t_s	Steel plate thickness [mm]
80	V_{GLT}	Volume of glulam for a truss [m ³]
81	V_{GLP}	Volume of glulam for a purlin [m ³]

82	x	Member of the study population
83	γ_m	Partial safety factor for a material property
84	ρ_m	Mean density [kg m^{-3}]

85 **Abbreviations**

86	AI	Artificial Intelligence
87	EC5	Eurocode 5 (CEN EN 1995-1-1: 2016)
88	GA	Genetic algorithm
89	GM	General Model
90	NLP	Nonlinear programming
91	SLS	Serviceability limit state
92	ULS	Ultimate limit state
93	2D	Two dimensions
94	2DGM	Two dimensions General Model
95	3D	Three dimensions
96	3DGM	Three dimensions General Model

97

98 **1. Introduction**

99 The use of heavy timber trusses is a common practice in construction to achieve large-
100 span roofs that also support the adjustment to a wide variety of shapes as well as
101 offering natural and aesthetic options for interior design. These large trusses are usually
102 comprised of elements made from glued laminated timber and mechanical joints, in
103 most cases, resolved with plates and dowel fasteners. This research work focuses on the
104 structural and cost optimisation of roofs made with such heavy timber trusses and
105 purlins, i.e. this paper aims to find the solution that meets the requirements of
106 functionality and security at the lowest possible cost. The need for the optimisation of
107 these structures arises from the calculation techniques employed by commercial
108 structural calculation programs (i.e. the independent dimensioning of bars and joints
109 that comply with the calculation standards), whereas the economic optimum could be
110 only achieved through general dimensioning algorithms. There are numerous structures
111 comprised of trusses and purlins that comply with the structural standards but the
112 challenge it is to put forward solutions (i.e. calculation schemes) that comply with the

113 standards while representing the lower possible cost. This research addresses the
114 necessary leap between the application of the corresponding structural standards and the
115 global cost-optimisation of a glued laminated timber roof structure.

116 Optimisation studies of structures are dated back to the 1970's, but in the last two
117 decades artificial intelligence (AI) techniques have been implemented (Houšť, Eliáš, &
118 Miča, 2013; McKinstry, Lim, Tanyimboh, Phan, & Sha, 2015) Among those
119 techniques, genetic algorithms (GA) are one of the most widely recognised and widely
120 employed in the optimisation of steel and concrete structures (Afshari, Hare, &
121 Tesfamariam, 2019; Cazacu & Grama, 2014; Dede, Bekiroğlu, & Ayvaz, 2011;
122 Fernandez, 2014; McKinstry et al., 2015; Park, Chun, & Lee, 2016; Prendes-Gero,
123 Bello-Garcia, del Coz-Diaz, Suarez-Dominguez, & Garcia-Nieto, 2018; Ruo-qiang,
124 Feng-cheng, Wei-jia, Min, & Yang, 2016). However, the optimisation of wooden
125 structures has not experienced the same level of attention from the scientific
126 community. Only a few references focused on timber frames could be found in the
127 literature (S. Šilih, Kravanja, & Premrov, 2010; Simon Šilih, Premrov, & Kravanja,
128 2005; Topping & Robinson, 1984), which predate the development of the current
129 Eurocodes for timber structures. The application of AI techniques in the study of timber
130 structures was pioneered by the authors, Villar, Vidal, Fernández, & Guaita, (2016), in a
131 paper addressing the optimisation of timber trusses through the programming of genetic
132 algorithms, which resulted in optimisation improvements when compared to earlier
133 methods. However, to the best of the authors' knowledge, there have been no significant
134 contributions in this line of work since then. This research takes a further step in the
135 optimisation of laminated timber structures by extending the optimisation to a three-
136 dimensional roof structure composed of glulam trusses on which purlins are arranged. It
137 is worth mentioning that contrary to the theoretical glulam cross-section approach

138 followed by previous studies (S. Šilih et al., 2010; Simon Šilih et al., 2005; Villar et al.,
139 2016) where a continuous variation of the cross-section dimensions was accepted and
140 any value could be selected, the optimisation method described in this paper was based
141 upon real glulam cross-section constraints, taking into account the laminate thicknesses
142 that are commercially available in the European market. Therefore, the thickness and
143 width of the boards employed to execute the glulam timber have been used which
144 implies that only discrete values of the cross-section dimensions could be selected
145 depending on the thickness and width of the timber boards. In the optimisation of this
146 type of timber structures, attention should be paid to numerous variables that impact on
147 the overall cost (number of joints, member cross-sections, number of fasteners, etc.) as
148 well as determine the structural design through their interaction in the different
149 structural members and at the 3D roof level, i.e. the spacing between trusses and purlins
150 should also be considered. In this regard, GAs have proven to be powerful tools when
151 multiple interacting variables are in play (Villar et al., 2016). Thus, a GA structural
152 optimisation procedure programmed in MATLAB (MathWorks, 2010) was carried out
153 in this paper.

154 Firstly, a two dimensional (2D) optimisation approach was performed where only the
155 timber trusses were considered in order to compare the results with those obtained by
156 the continuous optimisation implemented in Villar et al. (2016). Subsequently, the
157 optimisation of a complete roof was carried out by arranging purlins on the trusses to
158 obtain a three-dimensional structure (3D). Different truss spans and roof lengths were
159 studied, i.e. the separation between trusses and between purlins was added to the
160 structural optimisation and was incorporated as variables of the research. This allows, in
161 an innovative way, a more realist optimisation as the interaction between trusses,
162 purlins and joints was incorporated in overall cost of the structure.

163 Therefore, the 3D approach regarded the combined optimisation of separations, cross-
164 sections and joints, which is relevant due to the great importance of joints in the design
165 of heavy timber trusses (Villar-García, Crespo, Moya, & Guaita, 2018; Villar-García,
166 Vidal-López, Crespo, & Guaita, 2019). This experimental design also allowed for a
167 comparison between the 2D and 3D optimisations. Finally, a re-engineering of the
168 results was allowed in order to propose a pre-dimensioning method. In this way, the
169 costs resulting from the optimisation process were considered and the conclusions were
170 used to propose, in an unprecedented manner, a simplified method of optimum pre-
171 dimensioning.

172 **2. Timber roof structures. Structural calculation.**

173 This section addresses the structural calculation of roofs comprised of trusses and
174 purlins. Since the structural calculation of the trusses has already been reported by the
175 authors in a previous paper, only a summary is presented here with a more detailed
176 explanation to be found in Villar et al. (2016).

177 **2.1. Basic parameters**

178 The type of truss employed in this work, originally taken from Blass et al. (1995), was
179 the same used in Villar et al. (2016), which allowed a discrete and a continuous
180 optimisation of the truss cross-sections to be compared. Therefore, duo-pitch roof
181 trusses (Fig. 1) comprising of a horizontal bottom chord and two upper chords all
182 connected by vertical and diagonal intermediate members were assessed. The trusses
183 were classified depending on the number (n) of divisions that define the joints in the
184 upper chords as in Villar et al. (2016)..

Figure 1. Truss classification: (a) truss n6; (b) truss n10; (c) truss n14. Taken from Villar et al. (2016)

185 For three-dimensional optimisation, the roof structure was completed with purlins that
186 perpendicularly connected the trusses. The material of both the trusses and purlins was
187 GL32h glued laminated timber, so the mechanical properties specified in the CEN EN
188 14080 (2013) standard were adopted. In addition, a roof enclosure without structural
189 function was considered to take into account the load transferred to the structure.
190 Nevertheless, this roof enclosure was not included in the economic optimisation since
191 no variations in cost would result among the different cases of study.

192 **2.2. Ultimate Limit State (ULS) checks**

193 **2.2.1. Truss members**

194 The ultimate limit states (ULS) verification of cross-sections and members was
195 performed following the European standard of timber structures CEN EN 1995-1-
196 1:2016 (2016), hereinafter mentioned as Eurocode 5 or EC5.. A detailed explanation
197 could be found in Villar et al. (2016).

198 **2.2.2. Joints**

199 For the structures studied, the joints were defined by dowel fasteners and a steel plate as
200 the central member of a double shear connection. Regarding joint verification, the
201 equations specified in the EC5 (ec. 8.11 secc. 8.2.3 and ec. 8.34, secc. 8.6) were used to
202 assess the structural strength compliance. Nevertheless, it was also necessary to verify
203 the spacing between dowels as per EC5 requirements (Table 8.5, secc. 8.6). A detailed
204 explanation of the joints verification could be found in Villar et al. (2016).

205 **2.2.3. Purlins**

206 According to the EC5, the ULS check of purlins, which were considered simply
207 supported, involved the verification of the strength of the cross-section and the buckling

208 behaviour. Since the separation and length of the purlins were included as parameters in
209 the optimisation approach, the AI algorithm was responsible for applying the
210 corresponding loads as a function of those parameters. However, it was not necessary to
211 perform the calculation of any type of joint for the purlins, and only the presence of
212 support fittings in the trusses was considered to account for the cost effect.

213 **2.3. Serviceability limit state (SLS) checks**

214 The verification of the SLS implied checking the deflection in the middle of the span of
215 the truss and purlin. In the truss deflection, the slippage of its joints was considered
216 since it increases the deformation of the structure as observed by Villar et al. (2016). A
217 value of $l/300$ was selected, which is within the EC5 recommended range of limiting
218 values for the deformation (variable loads).

219 **2.4. Slipping of joints in ULS and SLS**

220 To incorporate the joint slippage in the SLS verification, an effective cross-section A_i^*
221 was considered according to Blass et al. (1995). The effective cross-section reduces the
222 real cross-section A_i of the structure members as a function of the member length, the
223 number of fasteners at both ends of the member, the mean value of the modulus of
224 elasticity (E_{mean}), the slip modulus (K_{ser}) in accordance with EC5, the timber mean
225 density and the fastener diameter, as previously indicated by Villar et al. (2016).

226 For the ULS verification, a similar effective cross-section expression was used to
227 incorporate the slippage by taking into account the ULS slip modulus, K_u ($K_u=2/3 K_{ser}$
228 as stipulated by EC5), and the 5% value of the modulus of elasticity, $E_{0.05}$.

229 **2.5. Structural design model**

230 In Villar et al. (2016) a structural 2D model was developed for the study of trusses, as a
231 first-order matrix calculation. The authors implemented a general model (GM) that used
232 rigid nodes except for the post and diagonals, which were considered pinned-pinned
233 elements, and considered the structure uniformly loaded. The GM exhibited a greater
234 level of accuracy. Therefore, the GM was used in this research work as it provides a
235 better representation of reality. Figure 2 shows the structural calculation model for both
236 the 2D optimisation, "truss model", and 3D optimisation, "truss and purling model", i.e.
237 simply supported purlins resting on the simply supported trapezoidal trusses.

Fig. 2. Structural calculation models: General truss Model and Purlins Model with boundary conditions.

238 **3. Optimisation parameters**

239 Two types of optimisation were carried out. Firstly, the trusses were studied as an
240 individual element, which resulted in an optimisation in two dimensions, i.e. in the
241 plane of the truss without considering the purlins, based on the general model (2DGM).
242 This approach enables drawing comparisons with the continuous optimisation carried
243 out by Villar et al. (2016) in order to serve both as a validation of the results and an
244 assessment of the influence of introducing a discrete optimisation, which is a more
245 realistic approach than the continuous hypothesis.

246 The second phase of this study examined the optimisation of trusses on which purlins
247 are arranged, i.e. a spatial structure constituting an entire roof. Therefore, the
248 optimisation was not limited to the sections of the structural elements but also included
249 the separations between the trusses and between the purlins (Fig. 2), which constituted a
250 3D optimisation (3DGM).

251 **3.1. Timber trusses to be optimised**

252 For the 2DGM optimisation, a truss of 22.5 m span, which corresponds to the one
253 optimised in Villar et al. (2016), was considered to enable further comparisons. In
254 addition, 15 and 30 m span trusses were also studied in the analysis of the entire roof
255 (3DGM optimisation). In this research work, the optimisation was based upon a cross-
256 section discrete approach, which recognises that the cross-section of the laminated
257 timber elements depends on the thickness and width of the boards employed in their
258 manufacture. In this regard, the most commonly used thicknesses employed in the
259 manufacture of glulam timber, which are 35, 40 and 45 mm, were used to obtain the
260 final height of the cross-sections, i.e. the height value was equal to a multiple of one of
261 those values. For the width of the pieces, 80, 100, 110, 130, 140, 160, 180, 200 and 220
262 mm are usual values (Argüelles, Arriaga, Esteban, Iñíguez, & Argüelles Bustillo, 2013).
263 Nevertheless, it should be noted that width values are greatly dependent on the
264 manufacturer, so values of 90, 120, 190 and 210 mm are also possible. Therefore, the
265 width range examined in this work oscillated between 90 and 220 mm in 10 mm
266 increments.

267 The geometry of the 22.5 m truss was originally described in Blass et al. (1995): a top
268 chord slope of 10° , raised eaves of $ht = 1$ m and a maximum depth at the ridge of $Ht =$
269 3 m (Fig. 1 and 3). In addition, the top chord was laterally restrained at a 3.8 m
270 separation as in the original truss. For the 15 and 30 m trusses, a scaling of the
271 previously described truss was performed as shown in Fig. 3. By following this
272 approach, the results were not affected by modifications in the structural typology and,
273 therefore, they were comparable.

Fig. 3. Geometry of the trusses considering a span of: 15 m, 22.5 m and 30 m. Example shown for type n10.

274 Regarding the uniform loads on the trusses, the ones described in Blass et al. (1995)
275 were also adopted: dead loads (2 kN m^{-1}) and snow loads (5 kN m^{-1}). Since the same

276 values were also employed by Villar et al. (2016) and Simon Šilih et al. (2005), a
277 comparison between the different 2D optimisations was possible. The weight of the
278 different structural elements was automatically entered by the algorithm according to
279 the cross-sections examined throughout the optimisation process. Furthermore, it was
280 considered a Service Class 2, a modification factor $k_{mod} = 0.9$, and a glulam safety
281 factor $\gamma_m = 1.25$.

282 At the joints, the same characteristics as those set in the aforementioned references
283 (Simon Šilih et al., 2005; Villar et al., 2016) were maintained to make the results
284 comparable: diameter of dowel $d = 14$ mm, thickness of the steel plate $t_s = 8$ mm,
285 structural steel grade S 235. A modification factor $k_{mod} = 0.9$ for short term load and
286 safety factor $\gamma_m = 1.3$ were used to calculate the dowels design load carrying capacity.
287 Then, the algorithm calculated and optimised the number of dowels in the joints. Since
288 a minimum height of the connected members is required depending on the number and
289 spacing between dowels, which has a clear implication in the minimum number of
290 laminates needed (Fig. 4), a 14 mm diameter of dowel was considered, which is the
291 minimum value usually employed in this type of trusses.

Fig. 4. Example of joint with dowel fasteners and minimum spacings following EC5.

292 **3.2. Roof structure to be optimised**

293 The 3D roof structure was comprised by the glulam trusses described in the previous
294 section and the purlins arranged between the trusses, which constitutes a common
295 structural solution for large open surfaces, e.g. livestock facilities, agro-industrial
296 warehouses or any other building in rural environments.

297 Regarding the dimensions of the roof, different widths were optimised (3DGM)
298 corresponding to the span of the trusses: 22.5 m, 15 m and 30 m, which are normal
299 values for this type of trusses. The roof structure was also optimised for different

300 lengths depending on the span: 1.5, 2 and 3 times the truss span were examined in order
301 to assess the influence of the amount of material in the trusses for the different lengths
302 (Fig. 5). The maximum length was limited to 3 times the span of the truss since
303 previous tests with greater lengths resulted in a practically constant cost per m^2 from
304 this point forward. The purlins were made of the same type glulam as the one employed
305 for the trusses, and the same assumptions about the laminate thickness and widths
306 indicated for the manufacture of the trusses were also considered for the purlins. They
307 were arranged as simply supported members between two adjacent trusses. It is to be
308 noted that, for the same study case, all elements of the structure were implemented with
309 the same laminate thickness.

Fig. 5. Roof structure to be optimised, example for truss type n10.

310 The 3DGM optimisation included everything indicated for the trusses but also included
311 the optimisation of the cross-sections, length and arrangement of the purlins. The length
312 of the purlins was considered a variable, which enabled the algorithm to select the
313 optimum separation between trusses to minimise the cost. Likewise, the variation of the
314 lateral separation between purlins was also allowed. For instance, the use of a roof cover
315 executed with wood sandwich panel with thermal insulation would allow a separation
316 between purlins ranging from 625 mm to 1250 mm, as long as the roof load allows such
317 variation. The top chord was considered laterally restrained at a length value equal to a
318 multiple of the separation between purlins, i.e. two times the separation in the 15 m
319 span truss, three times in the 22.5 m truss, and four times in the 30 m truss.

320 The surface loads applied in the 3DGM were similar to those indicated for the 2DGM
321 optimisation. However, in this case, the loads, were expressed in kN per m^2 so they
322 could be directly applied to the purlins depending on the different separation between
323 purlins and between trusses. Therefore, the following loads per m^2 were considered: a

324 dead load of 0.45 kN m^{-2} (it should be noted that this value does not account for the
325 weight of the purlins, which was introduced according to the cross-section resulting
326 from each step of the optimisation process) and a snow load of 1.25 kN m^{-2} , which is an
327 usual value in Europe. In this way, the value of the loads in the 2DGM model and in the
328 works of Blass et al. (1995), Simon Šilih et al. (2005) and Villar et al. (2016) would
329 imply a separation between trusses of 4 m, which constitutes an usual value in the
330 practice. Nonetheless, such value was not specified in none of those works as the
331 optimisations carried out were at the truss level, i.e. 2D. Furthermore, the wind effects
332 were only considered for the roof surface, since the side raised eaves and walls were
333 regarded as self-supporting without transmission of horizontal loads to the trusses. The
334 wind load was determined according to the European standard Eurocode 1, CEN EN
335 1194-1-4:2018 (2018), by taking into account a wind basic velocity pressure $q_b = 0.45$
336 kN m^{-2} , a terrain category II, an exposure factor $c_e(z) = 2.1$, and following the Eurocode
337 1 sections 4.2, 4.3, 4.5 and 7.2 to apply the pressure coefficients for buildings.

338 Table 1 summarises the optimisation parameters presented in this section.

339 **4. The Genetic algorithm optimisation**

340 The fundamentals of the genetic algorithms applied to timber structures have been
341 detailed in the authors' previous work and, thus, a more detailed explanation can be
342 found in Villar et al. (2016). So, this section only addresses the adaptation of the genetic
343 algorithms to this research work.

344 **4.1. Individuals**

345 Since two optimizations were made, it was required to establish two types of
346 individuals: "trusses" for the 2DGM optimisation, and "roofs", i.e. the roof structure
347 comprised of trusses and purlins, for the 3DGM optimisation.

348 **4.1.1. Individuals for the 2DGM optimisation**

349 Meanwhile the chromosomes encode the variables involved in the design (fasteners,
350 cross-sections, etc.) that define the individuals of the genetic algorithm, each individual
351 is a solution to the structural calculation.

352 The truss members were grouped for the same cross-section into three sets: top chord,
353 bottom chord, and intermediate (posts and diagonals) members according to their
354 structural performance. For the discrete optimisation, it was imposed that all elements
355 of a “truss” individual were required to have the same laminate thickness, i.e. 35, 40 or
356 45 mm as previously indicated. Furthermore, the individuals were coded according to
357 the number of laminates glued to achieve their final height (h) and their width (b)
358 according to the discrete values indicated in section 3.1. By following this discrete
359 approach, more realistic results than those obtained in the continuous optimization
360 carried out by Simon Šilih et al. (2005) and Villar et al. (2016) are to be expected.

361 Regarding the joints, the number of fasteners at the ends of a bar was allowed to vary
362 between 1 and 100. The optimal solutions would be those with the minimum number of
363 dowels and minimum steel plate surface while complying with the strength criteria.
364 Thus, the minimum required area for dowels placement also influenced the number of
365 laminates needed in the cross-section for the different thicknesses.

366 **4.1.2. Individuals for the 3DGM optimisation**

367 In the 3D optimisation, the chromosomes encoded both the dimensional characteristics
368 of the trusses, joints and purlins as well as their spatial arrangement and number.
369 Meanwhile each individual included both the previously described trusses and the
370 purlins used to connect them. A discrete optimisation was carried out and a constraint of
371 equal laminate thickness for all elements comprising the structure was imposed, which

372 is plausible since the entire structure would come from the same manufacturer. In the
373 optimisation of a surface defined by the span of the trusses and the length of the
374 building, the individual "roof" was constituted by a specific number of trusses and
375 purlins depending on their separation values, which were parameters added to the
376 optimisation. It is worth mentioning that, in this case, a continuous variation of the
377 separation values was allowed.

378 **4.2. The population**

379 The population size is important for the proper operation of the algorithm. Small
380 populations may impede the GA to reach the entire search space, whereas large
381 populations may involve high computational costs (Yang, 2014). In this work, two
382 different populations were examined according to the optimisation performed: the
383 population of "trusses" for the 2DGM optimisation and the population of "roofs" for the
384 3DGM optimisation.

385 For similar structural optimisations, several authors have employed populations ranging
386 from 60 to 250 individuals (Cazacu & Grama, 2014; Dede et al., 2011; Prendes Gero,
387 García, & del Coz Díaz, 2006; Toğan & Daloglu, 2006, 2008; Wang & Ohmori, 2013;
388 Yu, Li, Jia, Zhang, & Wang, 2015), but there have been instances in which up to 500
389 individuals have been examined (Dede et al., 2011; Talaslioglu, 2009; Wang & Ohmori,
390 2013). Regarding the population of "trusses", an initial population of 300 individuals
391 was considered in the previous work (Villar et al., 2016), the discrete optimisation
392 proposed in this paper entailed a finite number of possible cross-sections which limits
393 the need for large populations. Therefore, tests were conducted to reduce the 300
394 individuals and, thus, to increase computational efficiency without compromising the
395 exploration of the optimum. Finally, a 2DGM population consisting of 150 individuals
396 was considered throughout the entire optimisation, which was a similar value to the one

397 employed by Prendes-Gero et al. (2018, 2006) in the optimisation of concrete steel
398 profiles. The selected number of individuals resulted in a total runtime between 5 and
399 15 min running MATLAB as interpreted language and saving the results in a computer
400 Intel(R) Core(TM) i7 CPU 2.40GHz, 6.00GB RAM. The runtime depended on number
401 of truss members, but the time was around a 40-50 % of the time employed to reach the
402 optimum in a population of 300 individuals. From 150 individuals onwards, the number
403 of generations needed to reach the optimum is stabilised but the number of evaluations
404 of the objective function increases, which also rises the computational consumption
405 without offering improvements.

406 For the population of "roofs", a sensitivity study was carried out to determine the
407 number of individuals needed to reach the global optimum solution, taking into account
408 the new variables (purlins cross-sections, separations between trusses and between
409 purlins...), but without an excessive computational cost. Given the lack of previous
410 references in this regard, the sensitivity study considered populations between 150 and
411 500 individuals. Ultimately, it was found that a population comprised of 330 individuals
412 was required to reach the optimum, which required runtimes between 25 and 45 min
413 depending on the number of truss members as well as the different parameters
414 considered in each case. The selected number of individuals decreased the runtime
415 around 30-40 % compared to the initial population (i.e. 500 individuals). From 330
416 individuals onwards, the same rising behaviour identified in the 2D model was also
417 noticed, which advised against the increase of the population.

418 **4.3. The objective function**

419 In a genetic algorithm, the objective function or fitness function collects the variables
420 that intervene in the design in order to propose a value, such as volume of material, cost,
421 etc., that expresses the effectiveness of the design. Therefore, the optimal solution is

422 reached for the minimum value of the fitness function. In this work, two objective
 423 functions were defined: one for the optimisation of the trusses (2DGM) and other for
 424 the optimization of an entire roof (3DGM).

425 The objective function reflected both the cost of timber and the production cost of all
 426 the joints. For the 3DGM optimisation, the new costs associated to the purlins and the
 427 purlins hangers that were used to arrange the purlins on the trusses were also included.
 428 In addition, variables such as the span, number of trusses and purlins, separation
 429 between purlins were also considered to correctly determine the cost and, thus, the roof
 430 optimisation. Eq. (1) illustrates the objective function employed in the 3DGM
 431 optimisation:

$$432 \quad f(x) = (c_{tGL} \cdot V_{GLT} + c_{tdowel+steel} \cdot N_{dowels}) \times N_{trusses} + (c_{tGL} \cdot V_{GLP} + 2 \times c_{thanger}) \times N_{purlins} \quad (1)$$

433 where:

434 $f(x)$ manufacturing (material and labour) costs function of the structure [€];

435 c_{tGL} price of the manufactured and embedded timber material per m³, 900 [€
 436 m⁻³];

437 V_{GLT} volume of glulam in a truss [m³];

438 $c_{tdowel+steel}$ material cost and the manual labour costs per dowel for handling,
 439 assembling, drilling and bolting, including the adjoining steel plate, 2.5 [€
 440 dowel⁻¹];

441 N_{dowels} total number of dowels.

442 $N_{trusses}$ total number of trusses for a "roof" individual;

443 V_{GLP} volume of glulam for a purlin [m³];

444 ct_{hanger} material cost and the manual labour costs for handling and assembling
445 one purlin hanger, 3.75 [€ hanger⁻¹];

446 $N_{purlins}$ total number of purlins for a "roof" individual.

447 In the optimisation of an entire roof, the number of trusses $N_{trusses}$ and the number of
448 purlins $N_{purlins}$ were obtained by the algorithm in each case once the separation between
449 trusses and between purlins were defined. It is worth mentioning that the objective
450 function employed in the 2DGM optimisation coincides with the first addend of Eq. 1.

451 In order to compare the discrete and continuous optimisation approaches, the costs used
452 in the previous paper were also maintained for this work as they were considered to be
453 still valid.

454 In each generation, the haphazard creation of the population results in individuals who
455 do not meet the restrictions imposed by the calculation rules. The restricted problem is
456 converted to an unrestricted one by incorporating a penalty inside the objective function
457 (Yang, 2014). This penalisation could be conditional on the level of infringement of the
458 calculation rules. The modified objective function (Eq. 2) applied in the optimisation of
459 individual "trusses" (2DGM) is the same as the one defined by Villar et al. (2016):

$$460 \quad F(x) = f(x) + \sum_j [P_j(G_j(x))] + T(S(x)) \quad (2)$$

461 $F(x)$ modified objective function [€];

462 $f(x)$ cost objective function [€];

463 x individual of the study population;

464 j number of variable (member) studied;

465 $P_j(G_j(x))$ cost penalisation of the structure according to ULS as a function of
466 $G_j(x)$ [€];

467 $G_j(x)$ maximum utilisation ratio produced in each member j of individual x in
468 the ULS including checking fasteners. The utilisation ratio is the degree
469 of compliance of the ULS design conditions in a section – including the
470 check of the member's buckling instability. Higher values of $P_j (G_j(x))$
471 would imply that constraints are not satisfied, $G_j(x) > 1$ and $G_j(x) < 1$, so
472 the algorithm is required to adjust to the compliance limit.

473 $T(S(x))$ penalisation according to SLS as a function of $S(x)$ [€], it is a single
474 penalty for the whole truss. It is introduced so that $T(S(x))$ is calculated as
475 a function of $S(x) = \text{vertical deformation} / \text{deformation limit}$. Higher
476 values of $T(S(x))$ would imply that the constraints are not satisfied, $S(x) >$
477 1 and $S(x) < 1$, so the algorithm is required to adjust to the compliance
478 limit.

479 More details regarding $P_j (G_j(x))$ and $T(S(x))$ could be found in Villar et al.
480 (2016)

481 For the 3DGM optimisation, the modified objective function was similar to Eq. (2) but
482 also included two new terms to take into account the penalisation of the purlins
483 according to the ULS and SLS compliance.

484 This modified objective function was used to rank by fitness the individuals of a
485 generation.

486 **4.4. The reproduction operators**

487 Since the fundamentals of these operators have already been exposed by the authors
488 (Villar et al., 2016), this section addresses only the particularities pertaining to the
489 optimisation carried out in this paper, whereas more details on each operator could be
490 found in the aforementioned paper. To define the magnitude of the algorithm operators,
491 a sensitivity analysis was previously implemented by testing the set of values found in
492 the literature review. Finally, the selected values were those that led to improve the
493 efficiency achieved by the algorithm, and to guarantee that the algorithm would reach
494 the optimal solution.

495 **4.4.1. The selection and cross-over operators**

496 The roulette-wheel selection operator was used. This operator is characterized by a
497 proportionality to the fitness selection, which implies that more opportunities for
498 reproduction are given to the fittest individuals. In addition, the crossover operator
499 ensured the transmission of the characters among the best candidates. This research
500 work employed a two-point crossover, i.e. two points on the parents' chromosomes are
501 selected and the sections between those points are exchanged to create the offspring
502 chromosomes, since it has been demonstrated to be effective in the optimisation of the
503 trusses' cross-sections (Villar et al. 2016). The crossover probability defines the
504 population percentage that will take part in the crossover. For the optimisation of
505 individual trusses (2DGM), the previous sensitivity analysis indicated that a crossover
506 probability of 80% rendered the lowest result of the fitness function. For the
507 optimisation of entire roof (3DGM), the crossover percentage also remained effective at
508 the same value. Therefore, a 80% crossover probability was established for both
509 optimisations, which is in line with the values found in other works (Cazacu & Grama,
510 2014; Fernandez, 2014; Prendes-Gero et al., 2018; Villar et al., 2016).

511 **4.4.2. The elitism operator**

512 The elitism operator prevents the loss of the fittest individuals in subsequent
513 generations, which accelerates the optimisation. The elitism operator is established as a
514 percentage of the total. For the 2DGM optimisation of individual trusses, a 7 % elitism
515 percentage was selected after conducting a sensitivity study, which was slightly lower
516 than the one used in Villar et al. (2016). This discrepancy could be attributed to the
517 lower possibility of variation within the population given the discrete analysis of the
518 cross-sections. For the entire roof 3DGM optimisation, a 10 % elitism percentage was
519 selected after conducting a sensitivity study. Both values were in the range of those

520 found in the literature review (Cazacu & Grama, 2014; Fernandez, 2014; McKinstry et
521 al., 2015; Prendes-Gero et al., 2018).

522 **4.4.3. The mutation operator**

523 The mutation operator allows the algorithm to escape from local minima. This operator
524 alters components in the chromosomes of some individuals of the population. The
525 mutation positions in the chromosomes were selected at random. A previous sensitivity
526 study showed that a percentage of mutation of 1% (Villar et al., 2016) was the most
527 suitable for the optimisation of both trusses and the entire roof. This value was close to
528 those employed by other authors (Fernandez, 2014; Prendes-Gero et al., 2018; Prendes
529 Gero et al., 2006).

530 **4.4.4. The stopping criterion**

531 To conclude the optimisation process, the possible iterations were limited to 150
532 generations. However, it should be noted that a great number of calculations were
533 finished by convergence, which is achieved through 50 generations without
534 improvement and a 10^{-6} tolerance.

535 **5. Results and discussion**

536 **5.1. Optimisation of a single truss (2DGM). Comparison of the discrete and** 537 **continuous optimisation**

538 Table 2 shows the results obtained for the 22.5 m span truss in terms of volume of
539 timber, resulting cross-section, total number of dowels, instantaneous deflection
540 including the slip of the joints in the mid-span and cost. The table includes the results of
541 the three typologies of trusses ($n6$ $n10$ and $n14$) optimised through the discrete cross-
542 section approach for each laminate thickness, as well as to those obtained in the
543 continuous optimisation carried out by Villar et al. (2016). By comparing both
544 optimisation approaches, an increase in both the volume of timber and the cost was

545 observed when the discrete optimisation was applied. Nonetheless, it was observed that
546 the cross-sections obtained for the discrete and continuous optimisation were consistent
547 and reasonable for all cases and, thus, similar height to width ratios and total
548 dimensions were obtained.

549 The observation of all the results (Table 2) led to the following comments:

550 (i) Generally, the discrete optimisation adjusted the cross-section through width
551 increments to avoid increasing the cost by adding a higher number of laminates, which
552 represents a greater increase in cross-section area. In some cases, since a minimum
553 cross-section height is required to comply with the minimum spacing between the
554 dowels and between the dowels and the edges (Fig.4), the algorithm selected the
555 number of laminates that ensured the minimum height and, then, adjusted the width in
556 10 mm increments according to the needs of the cross-section. This approach seems a
557 more realistic calculation than that of the continuous optimisation, in which the
558 algorithm adjusts the height at the exact value required by the calculation and, at the
559 same time, the minimum width is also maintained. The difference is especially
560 noticeable for intermediate members, the discrete optimisation showed width (b)
561 increases before increasing the height by adding one more laminate.

562 (ii) The truss comprised of fewer number of elements (n_6) was the most economical for
563 all laminate thicknesses, as well as required lower volumes of timber. This result was
564 also observed for the continuous optimisation carried out by Villar et al. (2016).

565 (iii) The consideration of the laminate thickness implied an increase, on average, of 5.20
566 % in the volume of timber employed. Thus, the discrete approach triggered an average
567 cost increase of 2.59 % and a maximum rise of 6.20 % for the truss n_{14} . This cost
568 increase was a consequence of the increase in volume of timber since the cost of the

569 joints was not altered, on the contrary, the number of dowels was slightly reduced as a
570 result of the new cross-sections, Fig. 6.

571 *Fig. 6. Total cost (€) of a 22.5 m span truss depending on the laminate thickness and truss*
572 *typology. Comparison between the discrete approach and the continuous optimisation (C-OPT*
573 *from Villar et al., 2016)*

574 (iv) The laminate thickness influenced the cost and, in general, the 35 mm thickness
575 was the most economical solution. Although, 40 and 45 mm thicknesses resulted in
576 greater costs, no clear tendency between the cost increase and the thickness was
577 observed. Moreover, within each truss typology ($n6$, 10, 14), the cost increase as a
578 function of the thickness was variable. Nevertheless, the 35 mm thickness exhibited the
579 lowest increase when the discrete approach was compared to continuous optimisation
580 (Fig. 6), which implies a better capacity of adaptation to the continuous optimisation of
581 the cross-section. For the most economical truss, $n6$, and the smaller thickness, 35mm,
582 the discrete approach resulted in a cost increase of 1.12 % compared to continuous
583 optimization, the cross-section and the number of dowels were practically similar,
584 whereas a slightly higher volume of timber was required. These results indicated that
585 the discretisation of the cross-section to commercial thickness values may not imply a
586 large cost rise.

587 (v) For the discrete optimisation, the larger cross-sections and the reduced number of
588 dowels resulted in a slightly lower deflection values due to a diminished slippage of the
589 joints. In addition, in general, by increasing the laminate thickness used, deflections
590 were reduced as a consequence of the larger cross-sections at the same time greater
591 laminate thicknesses reduces the ability to approach the structural optimum.

592 (vi) Regarding the height to width ratios, values close to the unit (0.9 on average) were
593 noticed for the top chords, while the intermediate members and the bottom chord tended
594 to rectangular cross-sections and average values of 1.59 and 1.70 were observed

595 respectively. The top chords, that were subjected to compression, required greater width
596 values to resist the compressive buckling in the plane perpendicular to the truss, what
597 was not a limiting issue for the bottom chords or most of the intermediate members.
598 Such differences were also stated in the continuous optimisation and similar height to
599 width ratios were reported (Villar et al., 2016). However, for the intermediate members,
600 the rise of the cross-section area through the width increase instead of the height
601 increase by the addition of a new board prevented ratio values as high as in the
602 continuous optimisation. There was no thickness value that closely approximated the
603 height to width continuous ratios, i.e. a different thickness was best suited for a different
604 member type. Although, it should be pointed out that 35 and 40 mm thickness had the
605 closest fits.

606 No direct comparison between the discrete results and the nonlinear programming
607 (NLP) continuous optimisation carried out by Simon Šilih et al. (2005) was possible
608 since different standards were followed, i.e. versions and drafts previous to the current
609 Eurocode 5 (CEN EN 1995-1-1:2016, 2016) and to the current material characterization
610 norm (CEN EN 14080, 2013) were used in the NLP optimisation. Nonetheless, an
611 indirect connection could be performed by comparing the NLP vs the GA carried out by
612 Villar et al. (2016). The latter indicated cost improvements of 4.25 %, 7.49 %, and
613 13.44 % for n_6 , n_{10} and n_{14} trusses, respectively. Therefore, in spite of the cost
614 increase previously indicated between the discrete and to continuous optimisation, the
615 discrete approach still maintained a margin of cost reduction compared to the NLP
616 optimisation.

617 **5.2. Optimisation of an entire roof (3DGM)**

618 **5.2.1. Truss types for 3DGM optimisation**

619 The results of the 2DGM indicated that, for any laminate thickness studied, trusses
620 made of fewer members resulted in more economical solutions. In order to verify this
621 fact for the entire roof, a 3DGM optimisation was carried out for the intermediate
622 thickness, 40 mm, and the three types: *n6 n10 n14*. Similarly, trusses comprised of
623 fewer members were the most economical alternatives. Fig. 7 illustrates the cost per m^2
624 for the 22.5 m span truss and the three roof lengths considered: 1.5, 2 and 3 times the
625 span of the truss.

626 *Fig. 7. Cost (€ m^{-2}) for the 40 mm laminate thickness and 22.5m span (L) truss depending on the*
627 *truss typology and roof length (multiple of L).*

628 Based on the results, typology *n14* was disregarded due to its higher costs and the
629 subsequent 3D economic optimisation was focused on the *n6* and *n10* configurations of
630 the 22.5 m truss for the different laminate thicknesses. It was decided to address both
631 the *n6* and *n10* truss, to take into account the possibility that the joined consideration of
632 the truss typology and the thickness variation could alter the previous cost findings
633 when the optimization of the entire roof was considered.

634 Regarding the 15 m truss, the *n14* typology was also not studied since the resulting
635 dimensions of such configuration could not be considered as a heavy timber truss,
636 which is the structure examined in this paper. Thus, the initial study was carried out for
637 the *n6* and *n10* configurations of the 15 m truss and the intermediate board thickness, 40
638 mm. The results corroborated again the previous findings, the most economical option
639 lied in the use of the truss comprised of fewer members (Fig. 8). Therefore, the
640 subsequent optimisation study was only performed for the *n6* typology of the 15 m span
641 as a function of the board thickness (35, 40 and 45 mm).

642 *Fig. 8. Cost (€ m^{-2}) for 40 mm laminate thickness and 15m span (L) truss depending on the truss*
643 *typology and roof length (multiple of L) with 40 mm laminate thickness.*

644 For the 30 m span truss, a similar procedure was followed. In this case, typology n6 was
645 initially discarded due to lack of structural sense, since it would originate excessively
646 long and slender truss members. Thus, the initial comparison was performed for the n10
647 and n14 configurations of the 30 m truss and the intermediate thickness, 40 mm. In this
648 instance (Fig. 9), the results advised to carry out the optimisation study on the n10
649 typology of the 30 m span as a function of the board thickness (35, 40 and 45 mm).

650 *Fig. 9. Cost (€m²) for 40 mm thickness and 30m span (L) truss depending on the truss typology*
651 *and roof length (multiple of L).*

652 It is worth mentioning, that the selection of the trusses for the different optimisations
653 was not based solely on the aforementioned figures, as the decision was also supported
654 by the numerical results illustrated in Tables 3, 4, 5, 6 and 7, which constitute the
655 findings of the optimisation carried out in this research work and would be further
656 analysed in section 5.2.2.

657 **5.2.2. Discussion of 3D optimisation results**

658 In this section, the results of the optimisations carried out for the different truss
659 typologies, truss spans, roof lengths and laminate thickness studied are analysed. Tables
660 3, 4, 5, 6 and 7 show the resulting costs (total cost, cost of the trusses and cost of the
661 roof structure per m²) once each case was optimised. In addition, the tables also indicate
662 the structural characteristics of the solutions reached in each case: cross-sections of all
663 members, total m³ of timber, total number of dowels, separation of trusses and purlins,
664 as well as the instantaneous deflection at mid-span when the slip of the joints was
665 considered. Particularly, Tables 3, 4 and 5 illustrate the characteristics of the structural
666 optimum solutions depending on truss span and typology, roof length and laminate
667 thickness. Meanwhile, Tables 6 and 7 collect the non-optimal typologies, which were

668 employed in the selection of the truss typologies to be used in the final 3D optimisations
669 (section 5.2.1).

670 As an example of the optimisation process, Fig. 10 illustrates the evolution of the fitness
671 function of the 3DGM, i.e. the optimisation of the entire roof structure characterised by
672 a $n10$ truss typology, a 30 m span truss, a roof length equal to 3 times the span ($3 \times L$)
673 and a 45 mm board thickness. The decrease of the total cost towards the minimum value
674 occurred more steeply in the first generations. The optimal result was achieved after 46
675 iterations and, in this case, the process concluded by convergence, Haupt & Haupt
676 (2004) qualified this kind of behaviour as excellent. Cazacu & Grama (2014), Wang &
677 Ohmori (2013) and Ruo-qiang et al., (2016), who performed GA optimisations, also
678 reported a similar behaviour of the objective function. Conversely, a fewer number of
679 generations were necessary for convergence compared to the continuous optimisation in
680 Villar et al. (2016). The reduction in the number of generations (around 50%) was a
681 consequence of the width and height constraints of the possible cross-sections, i.e. due
682 to the discrete variation, which was especially significant for the 45 mm thickness.

683 *Fig. 10. Evolution of the fitness function of an entire rood characterised by a $n10$ truss*
684 *typology, a 30 m span truss, a roof length of 3 times the span ($3 \times L$) and a 45 mm laminate*
685 *board thickness.*

686 Finally, in order to further the discussion, the analysis of the results displayed in Tables
687 3, 4, 5, 6 and 7 prompted the remarks that could be observed in the following
688 subsections.

689 *5.2.2.1. Influence of truss span or roof width.*

690 For the same truss span, trusses comprised of fewer members were reported as the most
691 economical solution, which concurs with results obtained for the 2DGM optimisation.
692 As the truss type " n " increased, the truss contained a higher number of members and
693 joints and, thus, the cost of the structure also increased accordingly to the higher volume

694 of timber and number of joints per truss. Similarly, as the truss span increased, the surge
695 in cost per m^2 was accompanied by the increase in the cost percentage of the trusses on
696 the overall total cost, as a consequence of the greater volume of timber needed to cover
697 the larger span.

698 Regarding to the cross-sections, for the 15 m span truss (Table 3), the bottom chord and
699 the intermediate members tended to be optimised at the minimum width (i.e. 90 mm)
700 and the minimum height required due to dowel spacing according to EC5, i.e. the
701 minimum number of laminates that met the aforementioned limit. In the upper chords,
702 the width of the cross-sections was increased while the height remained at the minimum
703 number of laminates required by the arrangement of dowels, i.e. the algorithm obtained
704 the optimum by increasing the width in 10 mm increments up to 220 mm before
705 including one more laminate to the cross-section, which resulted in the use of greater
706 volumes of timber. Additionally, the width increases had a positive effect preventing the
707 buckling in the perpendicular direction to the truss.

708 As expected, 22.5 m span trusses also required greater cross-section areas (Table 4).
709 Whenever possible, the algorithm proposed a width increment instead of the increase in
710 the number of laminates. For the intermediate members and the bottom chord, the final
711 height often was determined by the minimum height required by the dowel spacing
712 requirement at the expense of greater width values. In fact, a similar behaviour was
713 noticed up to the 30 m span truss and, for most cases, no significant increases in the
714 height of the cross-sections were observed (Table 5). Conversely, for the upper chord,
715 the final height of the cross-section was usually higher than the minimum height
716 required by dowel spacing. Nonetheless, for some cases ($n10$ and $n14$ configurations of
717 22.5 m trusses), the final height coincided with the minimum requirement at values of
718 135, 140 and 160 mm, at the expense of higher height to width ratios (h/b), around 2.

719 For the 30 m span trusses, larger and quasi-quadrangular cross-sections were required in
720 the top chords.

721 For all cases, the deflection increased with the span but did not exceeded the SLS limit.

722 It is worth mentioning that, for a same truss span, the deflection increased for larger
723 values of truss type “ n ” due to the slippage effect of a greater number of joints.

724 *5.2.2.2. Truss separation*

725 The values reported for truss separation were among those commonly used in the
726 practice (between 4 and 4.5 m). This behaviour was especially noticed for trusses
727 comprised of fewer members and roof length equal to three times the truss span. For
728 instance, a separation between trusses of 4 m was proposed when a 40 mm laminate
729 thickness was employed, whereas a 4.5 m separation was reported for those trusses
730 made of 35 and 45 mm laminates. Nonetheless, some exceptions were observed for $n14$
731 trusses and recommendations for a 5 m truss separation appeared as the algorithm
732 attempted to reduce the volume of timber and, so, decrease the overall cost by reducing
733 the total number of trusses. Thus, for an increasing “ n ” type, the truss spacing also
734 tended to rise to counteract the volume increase added by a new truss, which was
735 especially significant from $n10$ to $n14$ type. The variation of the truss separation hardly
736 modified the cross-sections of the truss members. Nonetheless, separation values of 5 m
737 caused an increase in upper chord cross-sections while barely affected the intermediate
738 members or the bottom chord.

739 A similar behaviour was observed for the purlins, their cross-section hardly varied with
740 the separation between trusses and the purlins span, except for those cases resulting in
741 greater truss separations, 5 m, that also required greater height values in the cross-
742 sections. For most cases, the cross-sections of the purlins were optimised for the
743 minimum commercially-available width (90 mm), whereas the remaining purlins

744 required a 100 mm width. In any case, the height to width ratios were very similar,
745 ranging between 1.8 and 2. Nonetheless, some outliers were reported for trusses of
746 higher "n" and greater separation (height to width ratio =2.2.), or for a truss separation
747 lower than 4 m (height to width ratio =1.5).

748 *5.2.2.3. Purlin separation*

749 Regarding the separation between purlins, the algorithm always found the optimum at
750 the maximum admissible separation, i.e.1,250 mm. Since the addition of each new line
751 of purlins results in an important increase of timber, the algorithm always proposed the
752 minimum number of purlins to achieve the optimisation of the entire structure. The
753 behaviour exhibited by the algorithm corresponds to the usual procedure in the roof
754 construction, i.e. to separate the purlins as much as its allowed by the load and the roof
755 cover.

756 *5.2.2.4. Influence of roof length*

757 As the length of the roof increased, the cost per m² decreased slightly. Furthermore, the
758 influence of the cost of the trusses on the overall structure also was reduced. However,
759 this behaviour was less apparent when the 40 mm laminate thickness was employed.
760 The purlins cross-sections remained constant with the roof length increase due to the
761 small variation in the spacing between trusses. Nonetheless, as it has been already
762 indicated, a 10 mm increase in the width of the purlins was observed when the truss
763 separation reached 5 m. A similar behaviour was noticed for the truss members; small
764 differences were observed for the cross-sections of the upper chords due to the
765 variations in trusses separation. Conversely, in general, the cross-sections of the bottom
766 chord and the intermediates members remained constant.

767 Finally, it was observed that, in a roof with a length equal to three times the truss span,
768 the cost-effect of the initial and final trusses into the overall structure was diluted, which
769 could be considered equivalent to study an infinite roof length structure.

770 *5.2.2.5. Regarding to the laminate thickness*

771 The cost of the structure was affected by the selection of laminate thickness necessary to
772 fit the optimal theoretical cross-section, which was calculated according to both the
773 structural and dowel spacing requirements. In general, the results obtained for the
774 3DGM spatial optimisation confirmed the findings previously noticed in the 2DGM
775 optimisation.

776 Firstly, the variation in the laminate thickness did not affect the fact that the most cost-
777 effective solution is achieved by employing trusses comprised of fewer members.

778 For the same truss type and span, the laminate thickness modified the cost, and the 35
779 mm thickness resulted in the most economical alternative, followed by the 40 and 45
780 mm thickness. Although no clear trend was apparent, the 40 mm laminate resulted the
781 less economical thickness, especially when it was employed for the 15 and 30 m span
782 trusses. Thus, the 35 mm thickness exhibited the best fit to the theoretical cross-section
783 and the dowels spacing requirements. Figure 11 shows the cost of for the 15 m span
784 truss with the optimal typology, n6, according to Table 3. The timber volume was a
785 main factor on this behaviour followed by the influence of the number of dowels.

786 *Fig. 11. Total cost (€) of a 15 m span truss with optimal type n6*

787 Regarding the cross-sections, variations in the laminate thickness caused the following
788 behaviours:

789 - In the upper chord, for the same truss span and typology, the tendency observed
790 pointed to the use of a 35 mm laminate thickness to achieve lower cross-sections.

791 However, no similar trend was noticed for the other two thicknesses. In general, for roof

792 lengths equal to three times the truss span, the optimum was obtained with 4 laminates
793 for the 15 m truss and 5 - 6 laminates for the 22.5 and 30 m trusses, while the width of
794 the cross-section increased progressively with the span. In general, the highest height to
795 width ratios were obtained for the 40 mm thickness, whereas there was no clear trend
796 for the other two thicknesses.

797 - For the bottom chord, the increase in laminate thickness tended to rise the area of the
798 cross-section obtained through optimisation. Similarly, the height to width ratios also
799 increased for the same truss span and type when greater thicknesses were employed. In
800 general, for roof lengths equal to three times the truss span, the optimum was obtained
801 with 4 laminates and a width of 90 mm for the 15 m truss, 90-100 mm for the 22.5 m
802 truss and 120-130 mm for the 30 m truss.

803 - For the intermediate members, the largest cross-sections were obtained for the 40 mm
804 thickness, whereas similar cross-section values and height to width ratios were obtained
805 when the 35 and 45 mm laminates were employed. In general, the optimal solution was
806 reached, for roof lengths equal to three times the truss span, with a height of 3 laminates
807 for the 45 mm thickness and 4 laminates for 35 and 40 mm thickness, while the
808 optimum width followed a similar trend to that of the bottom chord.

809 The aforementioned tendencies indicated that the cross-sections and height to width
810 ratios of the bottom chord could be attributed to the algorithm that determined the width
811 and the number of laminates according to the structural requirements and no
812 modifications were needed thereafter since there was no need to stabilise the bottom
813 chord against buckling. However, the upper chords and intermediate members could be
814 subjected to buckling in the perpendicular direction to the truss span. Thus, the
815 algorithm had to adjust the width to avoid buckling and, at the same time, the height
816 through the number of laminates according to the board thickness. In this regard, it was
817 noticed that the 35 mm thickness resulted in the best fit to the minimum cross-section,

818 whereas the 45 mm and, especially, the 40 mm thickness exhibited more difficulties to
819 fit the calculated cross-section without exceeding the optimum. It should also be
820 mentioned that the determination of the cross-section in lower span trusses, was more
821 influenced by the minimum height necessary to comply with the dowel spacing
822 requirement than those of greater span, whose cross-section requirements easily
823 exceeded the limit imposed by the dowel spacing.

824 Furthermore, for trusses comprising of fewer members (i.e. optimal trusses) and roof
825 lengths equal to three times the truss span, the spacing between trusses (i.e. the length of
826 purlins) tended to 4.5 m for the 35 and 40 mm thicknesses, and 4 m for the 40 mm
827 thickness, which was in line with the previous finding that the 40 mm laminate offered
828 the worse economic results.

829 Regarding to the purlins, the thickness variation did not cause the algorithm to modify
830 the width cross-section, but the height was adjusted as much as possible. Although the
831 thickness increase rose the final cross-sections, no clear trends could be established as a
832 function of the laminate thickness. In addition, the laminate thickness had little effect on
833 the deflection values. In some cases, it was observed that the deflection was reduced
834 with the increase of the thickness. However, the variation also depended on the effect of
835 the final cross-sections reached for a specific thickness and purlin span.

836 **5.2.3 Construction cost per square meter**

837 Briefly, Table 8 shows all the results obtained through the economic optimisation,
838 expressed as euros per square meter of the roof structure, depending on the span and
839 typology of the trusses, the laminate thicknesses and the roof length.

840 As it can be observed in Table 8, the main aspects arising from this study are:

841 (i) the truss types comprised of fewer members resulted in the most economical
842 solutions.

843 (ii) the smaller laminate thickness, 35 mm, also generated the most economical results.
844 For the most cost-effective scenarios, i.e. trusses of fewer members, and roof length
845 equal to three times the truss span (equivalent to having infinite roof length), an average
846 cost saving around 3% was noticed when the 35 mm laminate thickness was employed.
847 Regarding the 40 and 45 mm thickness, none prevailed over the other as a better
848 alternative, Fig. 12.

849 *Fig. 12. Cost (€ m^{-2}) for the different truss span in the most cost-effective scenarios (i.e. selected*
850 *truss typology and roof length equal to three times the truss span).*

851 (iii) For the same truss types and laminate thickness, the increase of the length-to-span
852 decreased the cost due to the lower cost influence of the trusses in the entire structure.

853 **5.3. Differences between the individual trusses and the entire roof structure** 854 **optimisations**

855 Since the 3DGM optimisation was carried out for a variable spacing between trusses,
856 the results obtained could not be directly compared to those arising from the 2DGM
857 optimisation, as different loads were transmitted to the trusses in each model.
858 Nonetheless, it has been noticed that both the 2DGM and 3DGM approaches offered
859 similar results for the 22.5 m span trusses. For both cases, the most cost-effective
860 solution came from the trusses comprised of fewer members and made of the 35 mm
861 thickness. Moreover, the truss cost was similar, except for one case in which the 3DGM
862 optimisation exhibited a lower cost due to a lower truss separation than the 4 m
863 considered in the 2DGM, which resulted lower loads applied on the trusses, as well as
864 the different approach followed in each method to consider the weight of purlins, i.e. in
865 the 3DGM, the weight was automatically introduced by the algorithm as an exact figure

866 according to the specific cross-section, length and spacing for each iteration, whereas a
867 generic load was used in the 2DGM optimisation.

868 Regarding the dimensions of the elements comprising the trusses, similar height to
869 width ratios were reported for each set of members: upper chords, bottom chord and
870 intermediate members. The specific dimensions were also similar, although with small
871 variations in the cross-section height (± 1 laminate) as well as in the width due to the
872 different truss separation values.

873 Therefore, although both approaches have been considered valid, the 3DGM
874 optimisation produced better adjustments according to the authors' discretion.
875 Moreover, the 3DGM method provides more data to define the structure, since the
876 algorithm is the one responsible for finding out the optimum parameters, such as truss
877 typology, cross-sections, separation of purlins, separation of trusses, etc.

878 **5.4. Method for pre-dimensioning**

879 This section aims to state the general pre-dimensioning rules for glulam timber roof
880 structures similar to those studied in this work and subjected to loads close to those
881 established paper. Therefore, some guidelines on the general behaviour of the algorithm
882 were drawn.

883 Optimal results were analysed taking into account a roof length equal to three times the
884 truss span and the different values of truss span and board thickness studied in this
885 research work. The objective was to highlight the most significant or limiting
886 parameters and use them to construct simple equations that could assist an structural
887 engineer with the pre-dimensioning of a structure near to the optimum solution.
888 Nevertheless, it is worth mentioning that the recommended value should always be
889 inferior to the optimum to avoid exceeding it.

890 Firstly, the analysis of the aforementioned parameters allowed to set a series of rules for
891 the initial dimensioning of any truss span:

892 - Truss type: $n6$ for trusses up to 22.5 m and $n10$ for trusses over 22.5 m and up to 30 m.

893 - Regarding the cross-sections, the following considerations should be regarded: The
894 minimum commercial laminate width considered was 90 mm. The result of the pre-
895 dimensioning equations must be rounded to the immediate lower commercial width and
896 the number of laminates (n_{lam}) must be rounded to the nearest whole number. Then, the
897 starting height should be the minimum height required to comply with the dowel
898 spacing; initially, it may be considered two rows of dowels, but the final dowel
899 configuration would depend on the joint calculation. Subsequently, the following rules
900 would apply:

901 a) Purlins:

902 - Cross-sections; width (b): 90 mm; height (h): 5 laminates for a 35 mm thickness and 4
903 for a 40 and 45 mm thickness.

904 - Length of the purlins (which coincides with truss separation): 4 m for a 40 mm
905 thickness and 4.5 for a 35 and 45 mm thickness.

906 - Spacing between purlins: 1.25 m

907 b) Bottom chord, cross-sections:

908 - Height (h): 4 laminates, in all cases

909 - Width (b, mm): according to Eq. (3), where L (m) is the truss span:

$$910 \qquad \qquad \qquad b = 2.666 L + 46.66 \qquad \qquad \qquad (3)$$

911 c) Intermediate members, cross-sections:

912 - Heights (h): 3 laminates for a 45 mm thickness and 4 laminates for a 35 and 40 mm
913 thickness.

914 - Width (b, mm): according to Eq. (4), where L (m) is the truss span:

915
$$b = 2.222 L + 53.33 \quad (4)$$

916 d) Upper chord, cross-sections:

917 - Width (b , mm): according to Eq. (5), where L (m) is the truss span and L_r (mm) is the
 918 lateral restraining spacing:

919
$$b = \frac{Lr}{0.426 L + 11.26} \quad (5)$$

920 - Height (h): defined by the number of laminates (n_{lam}) according to Eq. (6) and (7):

921
$$n_{lam} = \frac{r}{0.016 r + 0.64} \quad (6)$$

922 Where r is:

923
$$r = \frac{L}{n} \quad (7)$$

924 and n is the number of divisions that define the joints in the upper chords (n_6 , n_{10} and
 925 n_{14}).

926 Table 9 shows the results obtained by the 3DGM and the pre-dimensioning rules for the
 927 structural calculation of an entire roof with a length equal to three times the truss span
 928 (which can be considered equivalent for a greater roof length due to the inalterability of
 929 the cost per m^2 from that point forward) and different truss span and board thickness.

930 As observed in Table 9, the number of laminates in the cross section obtained through
 931 the pre-dimensioning method coincided with the result proposed by the 3DGM
 932 optimisation for most cases. Nevertheless, for some cases in the top chord, the pre-
 933 dimensioning method resulted in a cross-section comprised of one less board, i.e. the
 934 optimum was not exceeded, which would be corrected in the subsequent calculations of
 935 the structure. Regarding the widths of the cross-sections, variations were observed for
 936 some cases and the pre-dimensioning method indicated values that differed, on average,
 937 by less than 8%. However, an outlier was noticed for the n_6 configuration of the 15 m
 938 span truss. Only at one point in the upper chord, the width exhibited a greater

939 difference, around 15%, due to a greater variability in the cross-section proposed by
940 each optimisation technique. Nevertheless, the proposed method resulted in a reliable
941 approach to obtain pre-dimensioning results close to the structural optimum, which
942 logically does not exempt the structure to undergo a detailed final calculation to ensure
943 the compliance with the established calculation rules.

944 **6. Conclusions**

945 The GAs have proven to be a valid method to optimise glued laminated timber
946 structures when the laminate thickness is considered. The optimisation was carried out
947 successfully both at the truss level (2D) and the roof structure level (3D). Moreover, it
948 was revealed that the most realistic and appropriate procedure for optimising glulam
949 structures is to take into account the actual thickness and width of the laminates boards
950 of timber.

951 For the 2D optimisation, the GA obtained the best solutions at an initial population of
952 150 individuals, an elitism operator of 7%, a crossover probability of 80 % and
953 mutation rate of 1%. Similarly, the best solutions in the 3D model were obtained for an
954 initial population of 330 individuals, an elitism operator of 10%, a crossover probability
955 of 80 % and mutation rate of 1%. The comparison between the 2D discrete optimization
956 and the continuous optimisation reported by Villar et al. (2016) has led to the following
957 conclusions:

958 - The most economical solutions were also obtained when trusses comprised of fewer
959 members were considered.

960 - The best cost results were obtained for the smaller laminate thickness, 35 mm.

961 - For the most economical truss, n6 and 35 mm laminate thickness, the cost increase
962 obtained in the discrete approach was only 1.12% higher compared to the continuous
963 optimisation, which resulted in a mostly similar cross-sections for both models.

964 - It was observed that the use of the Genetic Algorithms optimisation resulted in lower
965 costs than those obtained through NLP (non-linear programming), (Simon Šilih et al.,
966 2005), even when the laminate thickness was taken into account in the GA model.

967 Regarding the 3D discrete optimization for an entire roof structure, the results obtained
968 have led to the following conclusions:

969 - In a spatial roof structure as the one described in this work, the use of trusses
970 comprised of fewer members also rendered the most economic solutions.

971 - Similarly, the best economical results were obtained for the smaller laminate
972 thickness, 35 mm.

973 - In terms of truss separation, it was observed that the GA proposed values commonly
974 used in the practice, i.e. 4 m for a 40 mm laminate thickness and 4.5 m for laminate
975 thickness of 35 and 45 mm.

976 - Regarding the separation between purlins, the algorithm always found the optimum at
977 the maximum allowed separation, which is consistent with the usual execution
978 procedure of roof structures with purlins.

979 - Depending on the laminate thickness, recommendations for typology, members cross-
980 sections and spacing between trusses and purlins may be proposed in order to obtain
981 optimised glulam roof structures. Therefore, a simplified method of pre-dimensioning
982 has been proposed to obtain a 3D structural arrangement close to the optimum.

983 - The authors consider the 3D optimisation represents the preferred alternative to set the
984 optimum design and cost adjustment for the roof timber structures.

985 **Acknowledgments**

986 Partial support from the Junta de Extremadura (Spain) through Grants no.
987 GR18175 and GR18193 (partially financed by FEDER funds) is gratefully
988 acknowledged.

989 **REFERENCES**

- 990 Afshari, H., Hare, W., & Tesfamariam, S. (2019). Constrained multi-objective optimization
991 algorithms: Review and comparison with application in reinforced concrete structures.
992 *Applied Soft Computing*, 105631. <https://doi.org/10.1016/J.ASOC.2019.105631>
- 993 Argüelles, R., Arriaga, F., Esteban, M., Iñíguez, G., & Argüelles Bustillo, R. (2013). *Timber*
994 *Structures. Basis for Calculation (in Spanish)*. Madrid, Spain: AITIM. Technical Research
995 Association of the Wood and Cork Industries.
- 996 Blass, H. J., Aune, P., Choo, B. S., Görlacher, R., Griffiths, D. R., Hilson, B. O., et al. (1995).
997 *Timber engineering STEP2. Design -details and structural systems*. Almere, The
998 Netherlands: The Centrum Hout.
- 999 Cazacu, R., & Grama, L. (2014). Steel Truss Optimization Using Genetic Algorithms and FEA.
1000 *Procedia Technology*, 12, 339–346. <https://doi.org/10.1016/j.protcy.2013.12.496>
- 1001 CEN EN 1194-1-4:2018. (2018). *Eurocode 1 : Actions on structures - Part 1.4: General actions*
1002 *-Wind actions*. Brussels, Belgium: European Committee for Standardisation.
- 1003 CEN EN 14080. (2013). *Timber structures. Glued laminated timber and glued solid timber.*
1004 *Requirements*. Brussels: European Committee for Standardisation.
- 1005 CEN EN 1995-1-1:2016. (2016). *Eurocode 5 : Design of timber structures - Part. 1.1 General.*
1006 *Common rules and rules for buildings*. Brussels, Belgium: European Committee for
1007 Standardisation.
- 1008 Dede, T., Bekiroğlu, S., & Ayvaz, Y. (2011). Weight minimization of trusses with genetic

1009 algorithm. *Applied Soft Computing*, 11(2), 2565–2575.
1010 <https://doi.org/10.1016/j.asoc.2010.10.006>

1011 Fernandez, M.-S. (2014). *Optimización de estructuras de invernadero por algoritmos genéticos*.
1012 PhD Thesis. Faculty of Agricultural Engineering, University of Extremadura, Spain.

1013 Haupt, Randy L.; Haupt, Sue E. (2004). *Practical Genetic Algorithms* (2nd ed.). New Jersey:
1014 John Wiley & Sons.

1015 Houšť, V., Eliáš, J., & Miča, L. (2013). Shape optimization of concrete buried arches.
1016 *Engineering Structures*, 48, 716–726. <https://doi.org/10.1016/j.engstruct.2012.11.037>

1017 MathWorks. (2010). Matlab. Massachusetts.

1018 McKinstry, R., Lim, J. B. P., Tanyimboh, T. T., Phan, D. T., & Sha, W. (2015). Optimal
1019 design of long-span steel portal frames using fabricated beams. *Journal of Constructional*
1020 *Steel Research*, 104, 104–114. <https://doi.org/10.1016/j.jcsr.2014.10.010>

1021 Park, J., Chun, Y.-H., & Lee, J. (2016). Optimal design of an arch bridge with high performance
1022 steel for bridges using genetic algorithm. *International Journal of Steel Structures*, 16(2),
1023 559–572. <https://doi.org/10.1007/s13296-016-6024-y>

1024 Prendes-Gero, M.-B., Bello-Garcia, A., del Coz-Díaz, J.-J., Suarez-Dominguez, F.-J., & Garcia-
1025 Nieto, P.-J. (2018). Optimization of steel structures with one genetic algorithm according
1026 to three international building codes. *Revista de La Construcción*, 17(1), 47–59.
1027 <https://doi.org/10.7764/RDLC.17.1.47>

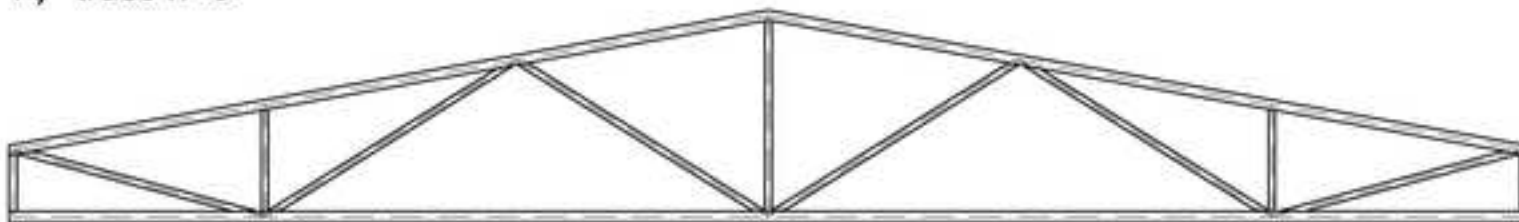
1028 Prendes Gero, M. B., García, A. B., & del Coz Díaz, J. J. (2006). Design optimization of 3D
1029 steel structures: Genetic algorithms vs. classical techniques. *Journal of Constructional*
1030 *Steel Research*, 62(12), 1303–1309. <https://doi.org/10.1016/j.jcsr.2006.02.005>

1031 Ruo-qiang, F., Feng-cheng, L., Wei-jia, X., Min, M., & Yang, L. (2016). Topology
1032 Optimization Method of Lattice Structures Based on a Genetic Algorithm. *International*

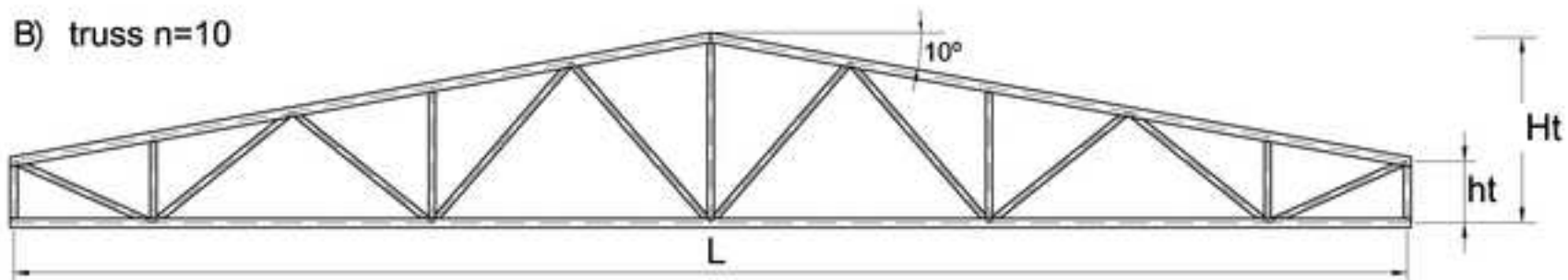
- 1033 *Journal of Steel Structures*, 16(3), 743–753. <https://doi.org/10.1007/s13296-015-0208-8>
- 1034 Šilih, S., Kravanja, S., & Premrov, M. (2010). Shape and discrete sizing optimization of timber
1035 trusses by considering of joint flexibility. *Advances in Engineering Software*, 41(2), 286–
1036 294. <https://doi.org/10.1016/J.ADVENGSOFT.2009.07.002>
- 1037 Šilih, Simon, Premrov, M., & Kravanja, S. (2005). Optimum design of plane timber trusses
1038 considering joint flexibility. *Engineering Structures*, 27(1), 145–154.
1039 <https://doi.org/10.1016/J.ENGSTRUCT.2004.10.001>
- 1040 Talaslioglu, T. (2009). A new genetic algorithm methodology for design optimization of truss
1041 structures: Bipopulation-based genetic algorithm with enhanced interval search. *Modelling
1042 and Simulation in Engineering*, 2009. <https://doi.org/10.1155/2009/615162>
- 1043 Toğan, V., & Daloğlu, A. T. (2006). Optimization of 3d trusses with adaptive approach in
1044 genetic algorithms. *Engineering Structures*, 28(7), 1019–1027.
1045 <https://doi.org/10.1016/j.engstruct.2005.11.007>
- 1046 Toğan, V., & Daloğlu, A. T. (2008). An improved genetic algorithm with initial population
1047 strategy and self-adaptive member grouping. *Computers & Structures*, 86(11–12), 1204–
1048 1218. <https://doi.org/10.1016/j.compstruc.2007.11.006>
- 1049 Topping, B. H. V., & Robinson, D. J. (1984). Optimization of timber framed structures.
1050 *Computers & Structures*, 18(6), 1167–1177. [https://doi.org/10.1016/0045-7949\(84\)90161-](https://doi.org/10.1016/0045-7949(84)90161-5)
1051 5
- 1052 Villar-García, J. R., Crespo, J., Moya, M., & Guaita, M. (2018). Experimental and numerical
1053 studies of the stress state at the reverse step joint in heavy timber trusses. *Materials and
1054 Structures*, 51(1), 17. <https://doi.org/10.1617/s11527-018-1144-9>
- 1055 Villar-García, J. R., Vidal-López, P., Crespo, J., & Guaita, M. (2019). Analysis of the stress
1056 state at the double-step joint in heavy timber structures. *Materiales de Construcción*, *In
1057 press.*

- 1058 Villar, J. R., Vidal, P., Fernández, M. S., & Guaita, M. (2016). Genetic algorithm optimisation
1059 of heavy timber trusses with dowel joints according to Eurocode 5. *Biosystems*
1060 *Engineering*, *144*, 115–132. <https://doi.org/10.1016/j.biosystemseng.2016.02.011>
- 1061 Wang, H., & Ohmori, H. (2013). Elasto-plastic analysis based truss optimization using Genetic
1062 Algorithm. *Engineering Structures*, *50*, 1–12.
1063 <https://doi.org/10.1016/j.engstruct.2013.01.010>
- 1064 Yang, X.-S. (2014). *Nature-Inspired Optimization Algorithms*. London: Elsevier.
1065 <https://doi.org/10.1016/B978-0-12-416743-8.00016-6>
- 1066 Yu, W., Li, B., Jia, H., Zhang, M., & Wang, D. (2015). Application of multi-objective genetic
1067 algorithm to optimize energy efficiency and thermal comfort in building design. *Energy*
1068 *and Buildings*, *88*, 135–143. <https://doi.org/10.1016/j.enbuild.2014.11.063>
- 1069

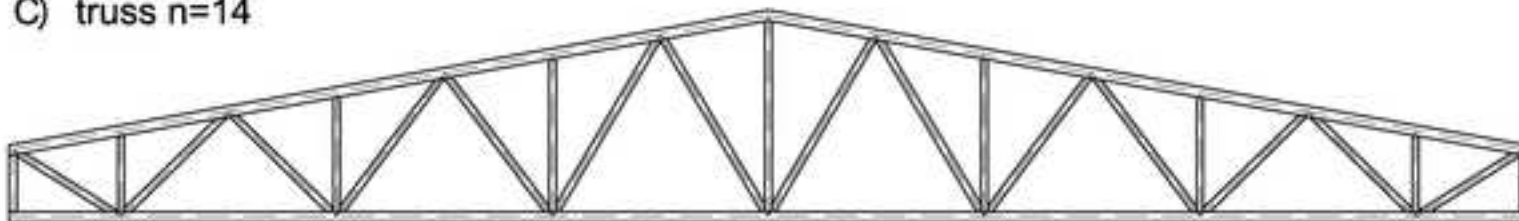
A) truss n=6



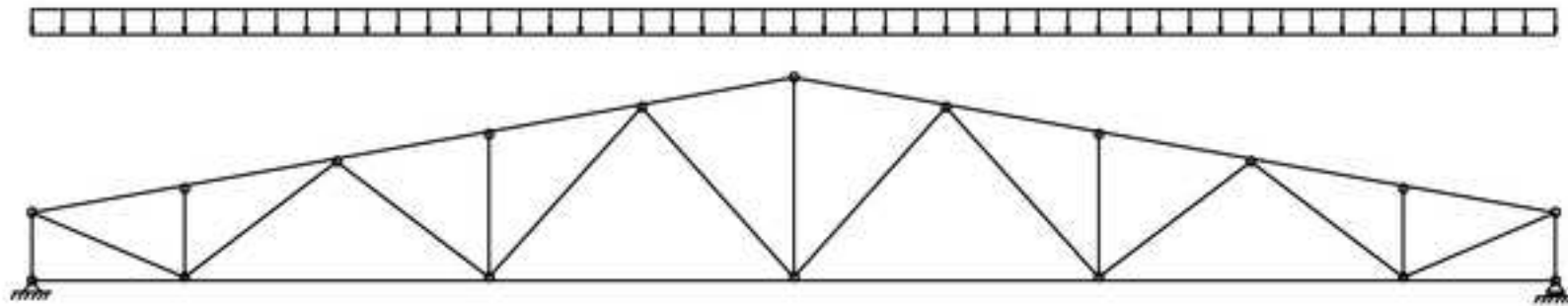
B) truss n=10



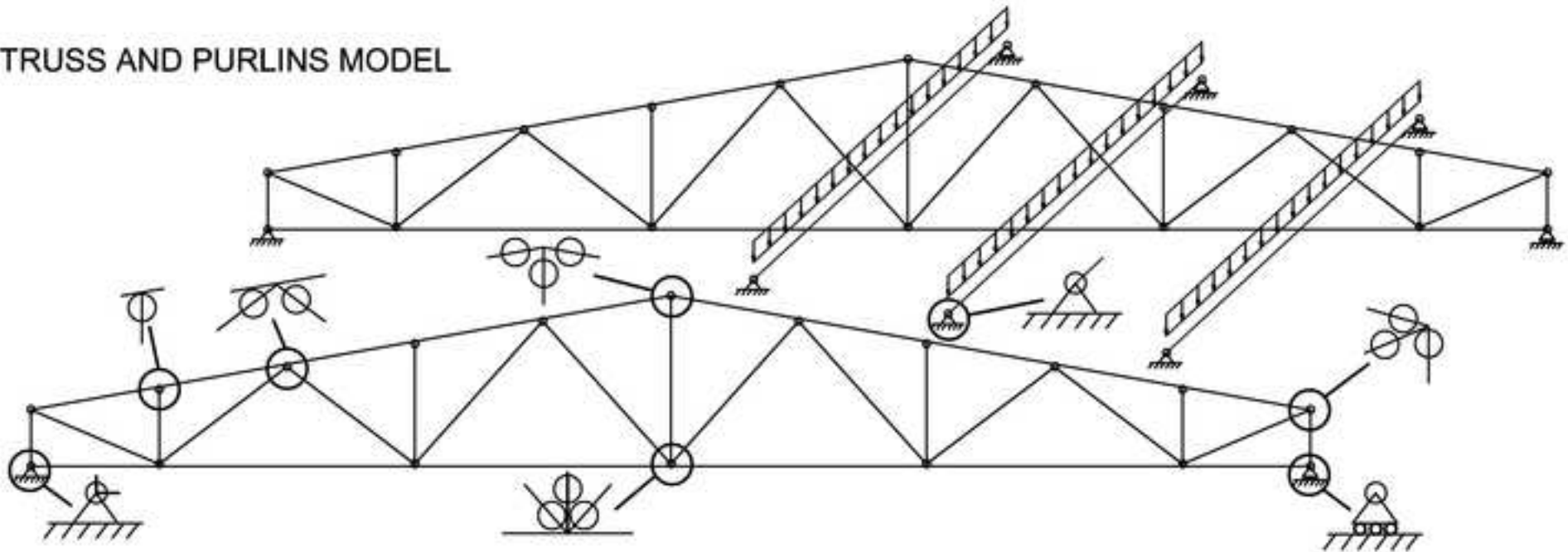
C) truss n=14

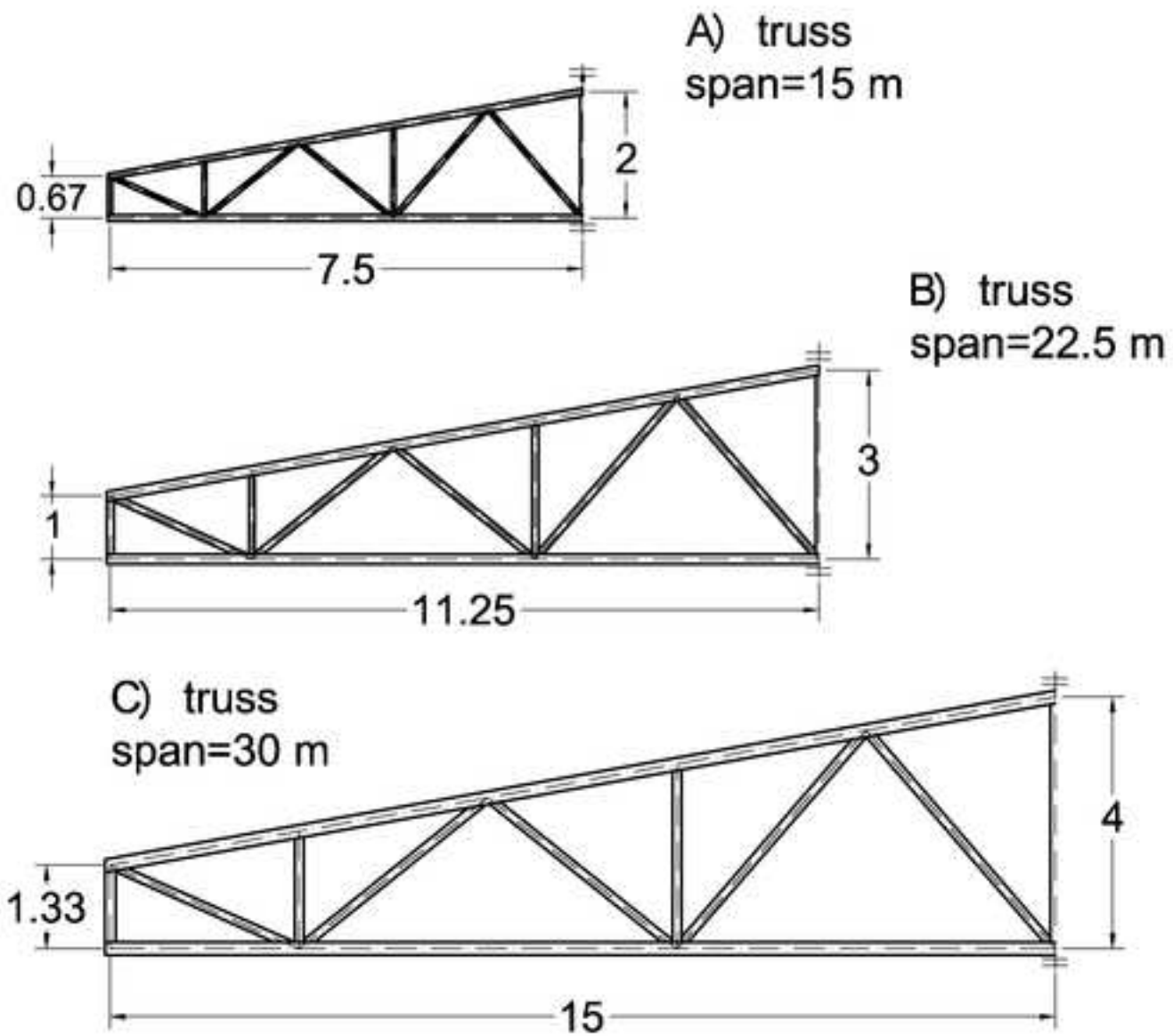


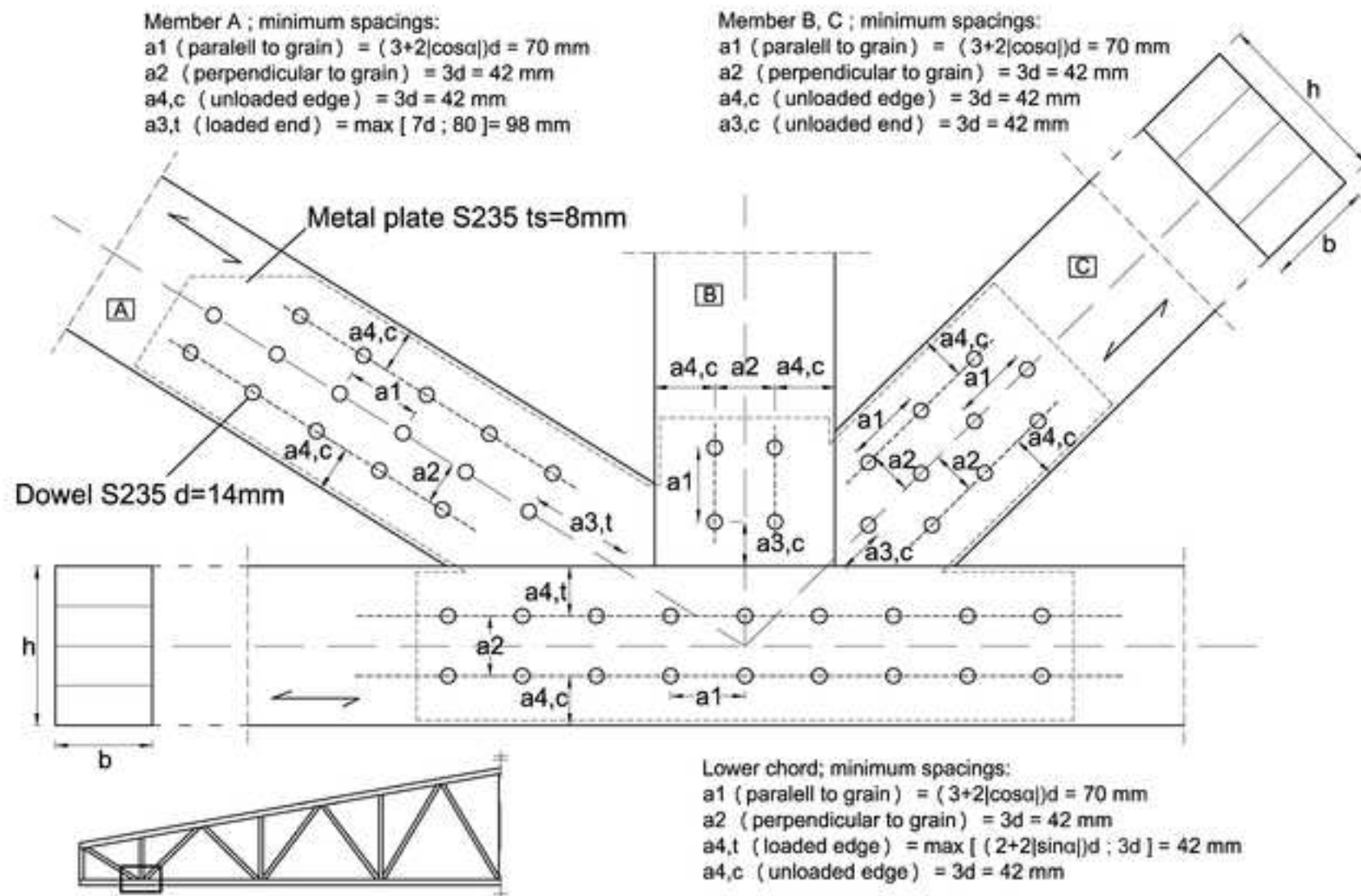
TRUSS MODEL (GENERAL MODEL)

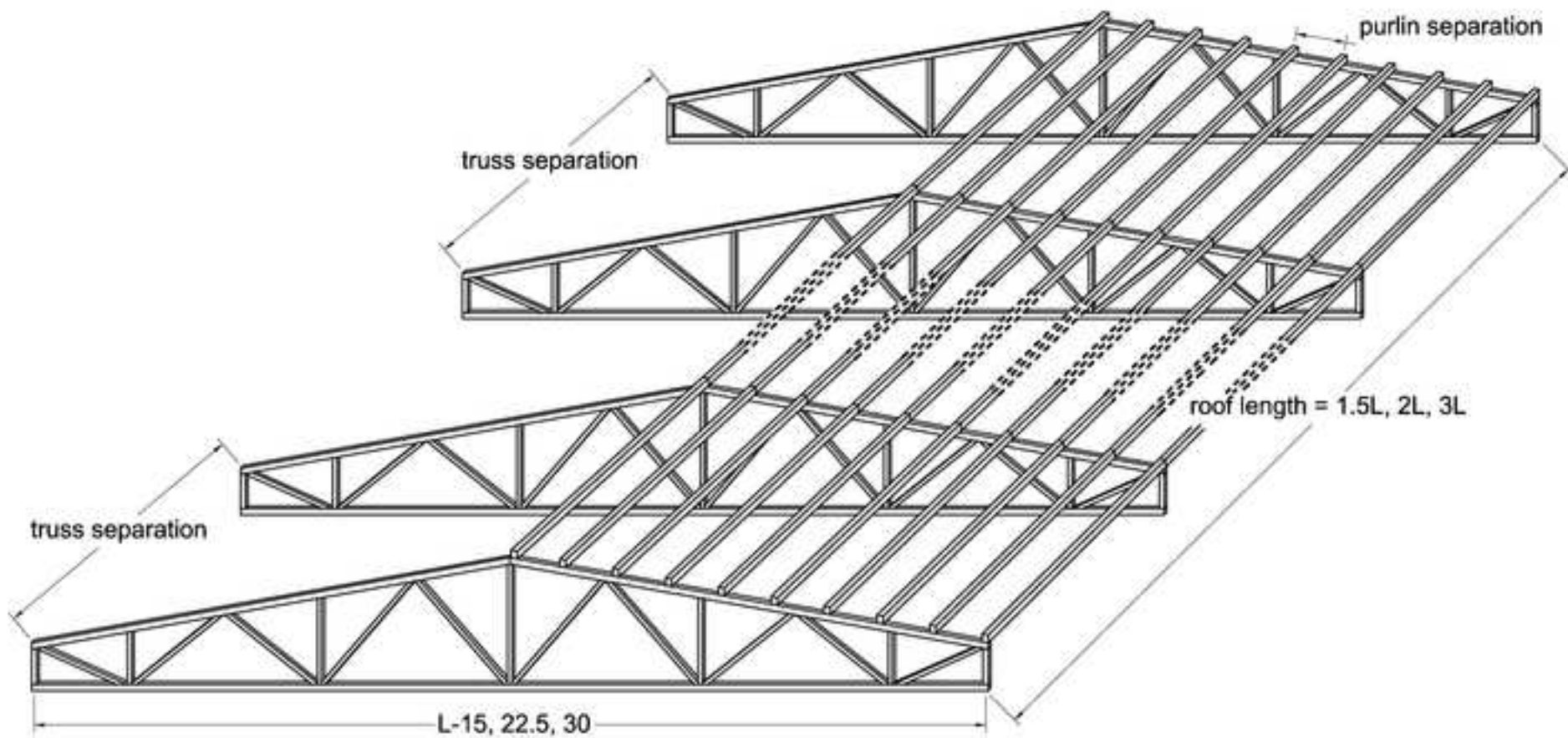


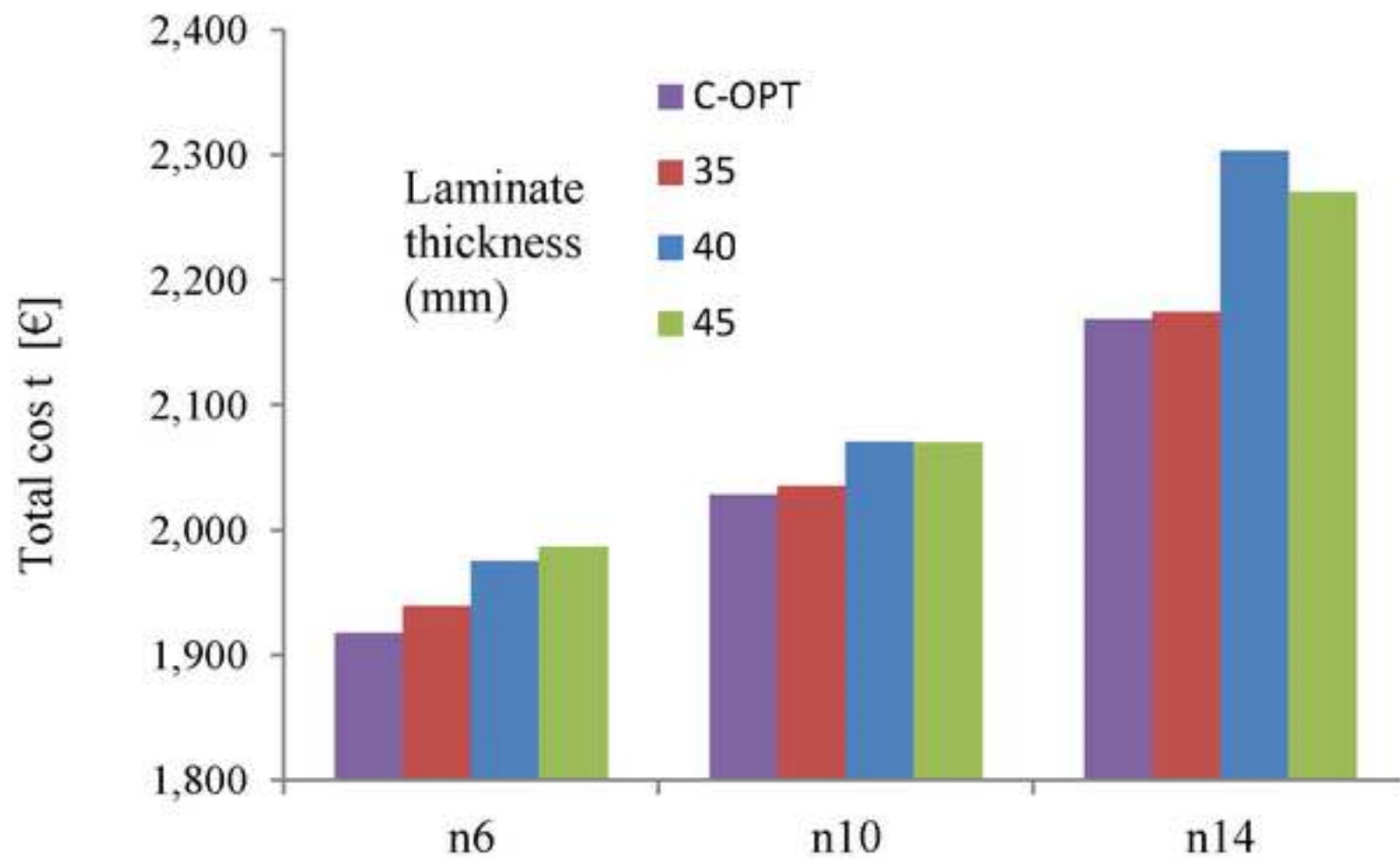
TRUSS AND PURLINS MODEL

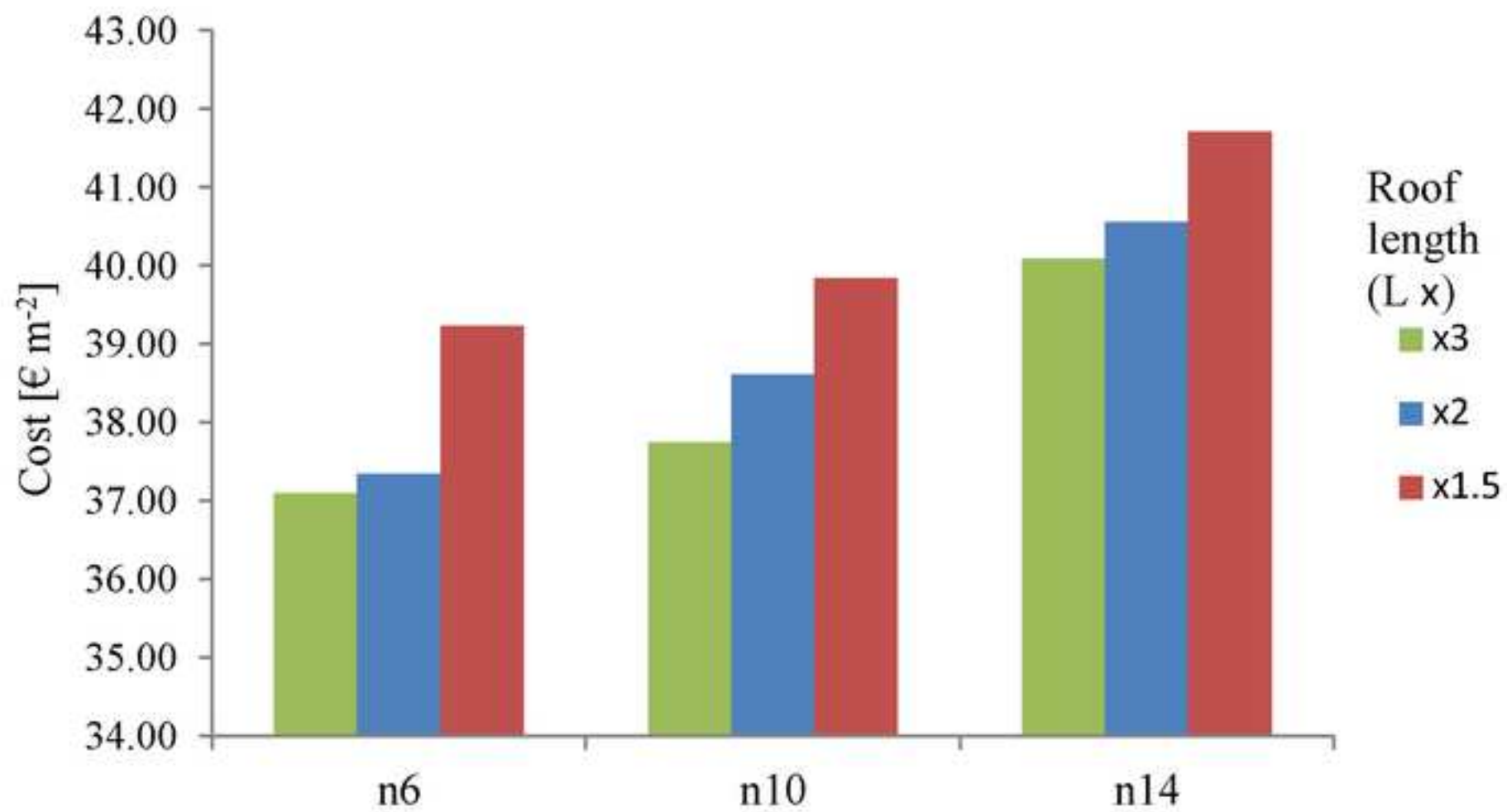


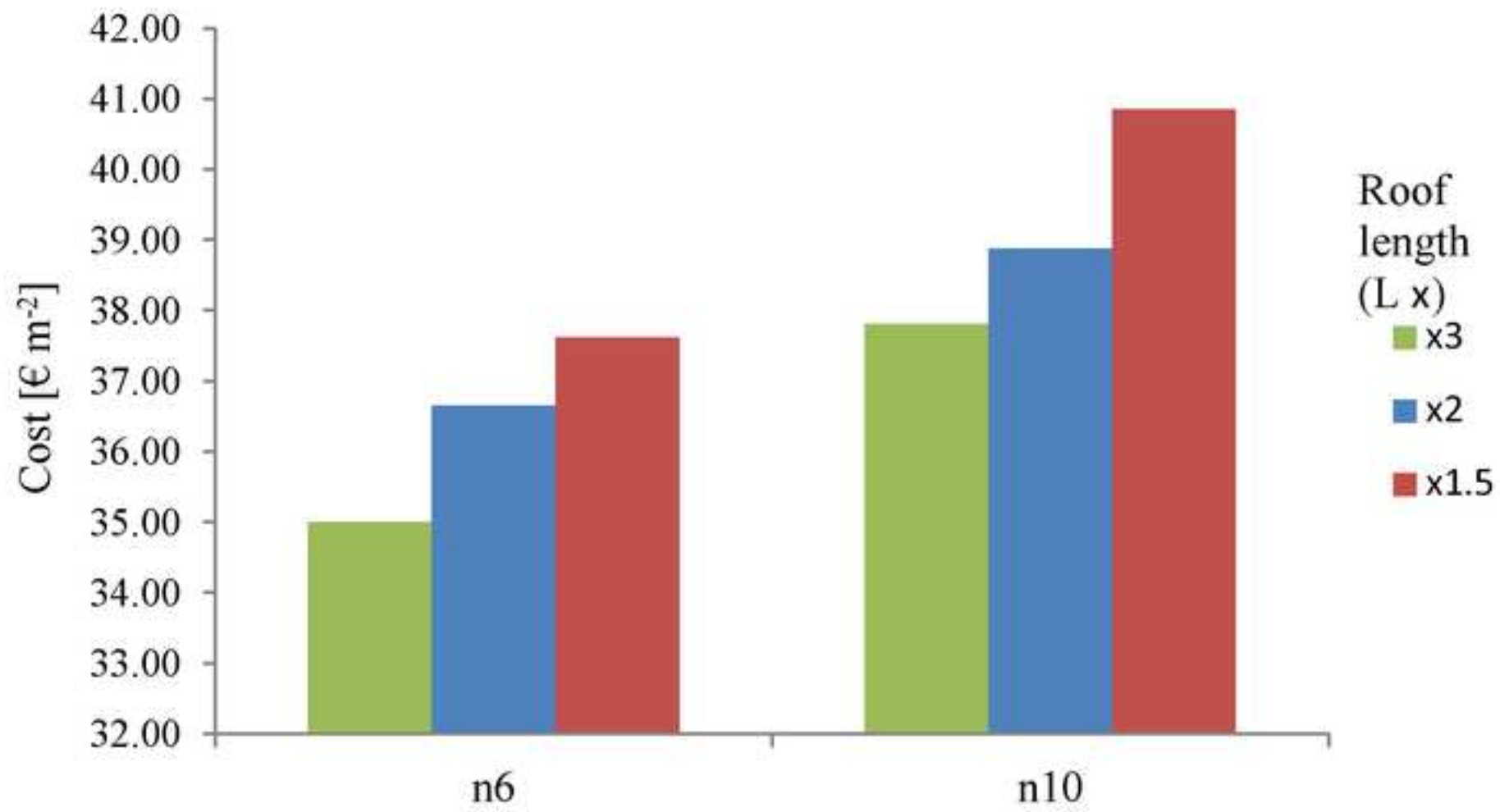


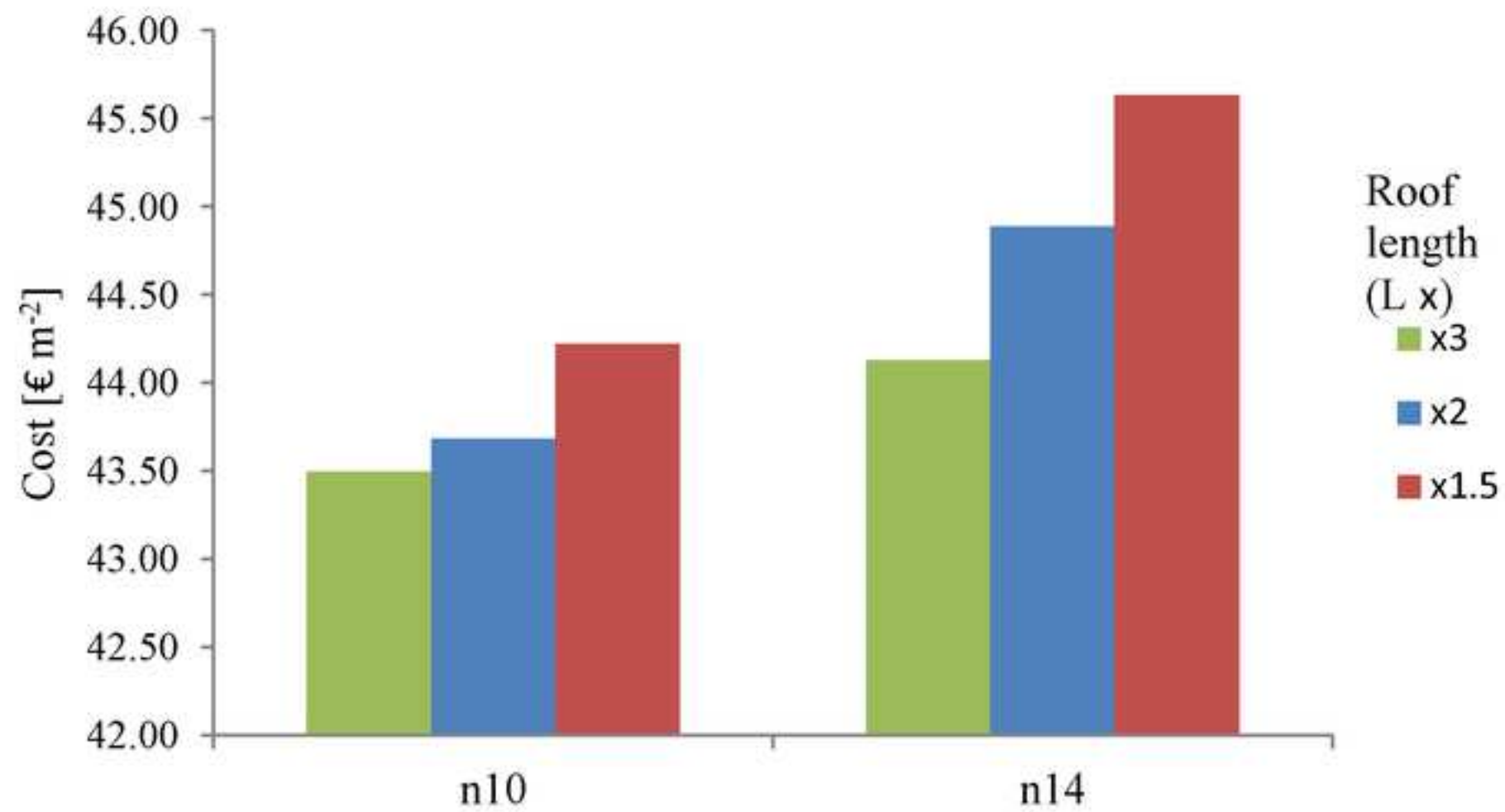


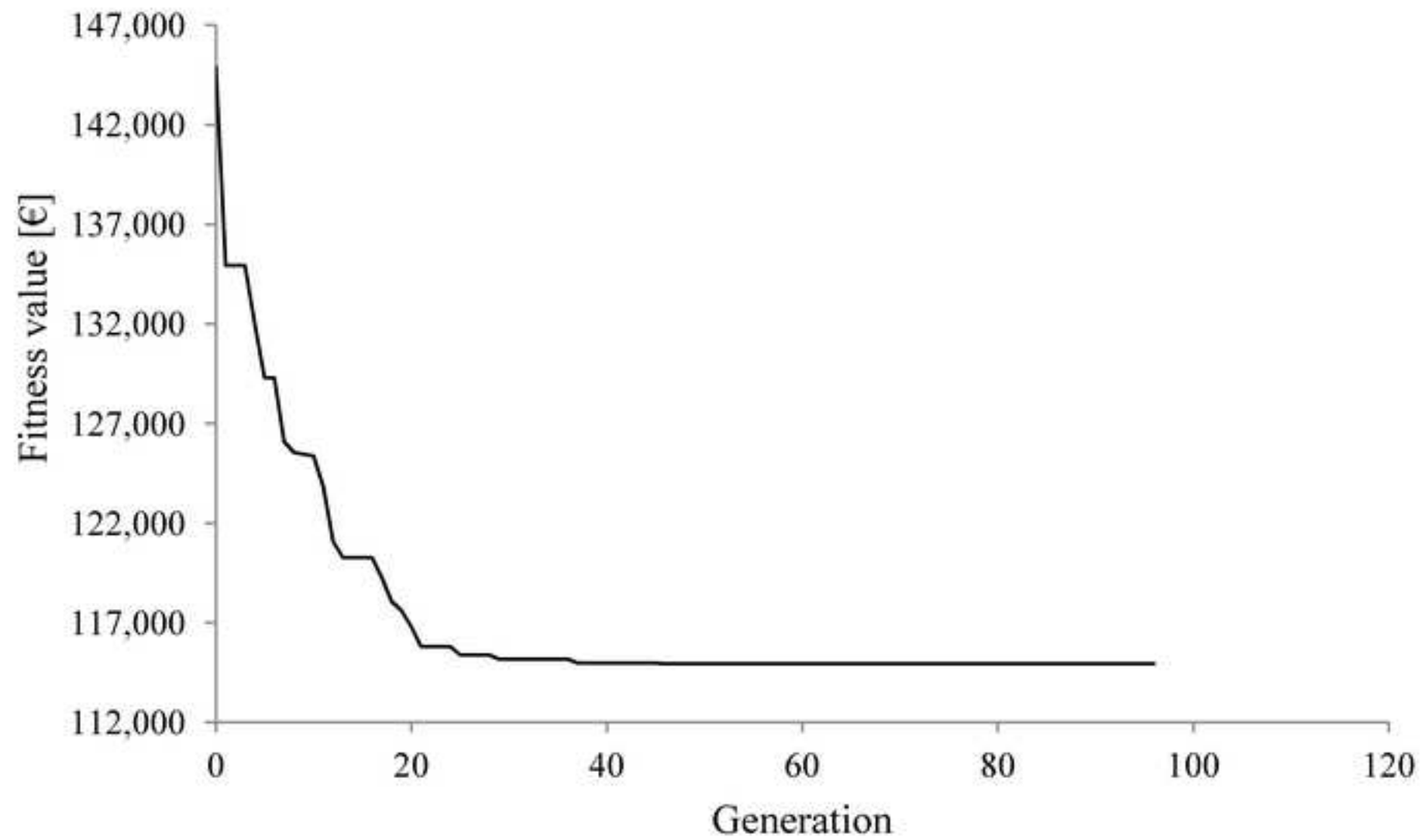


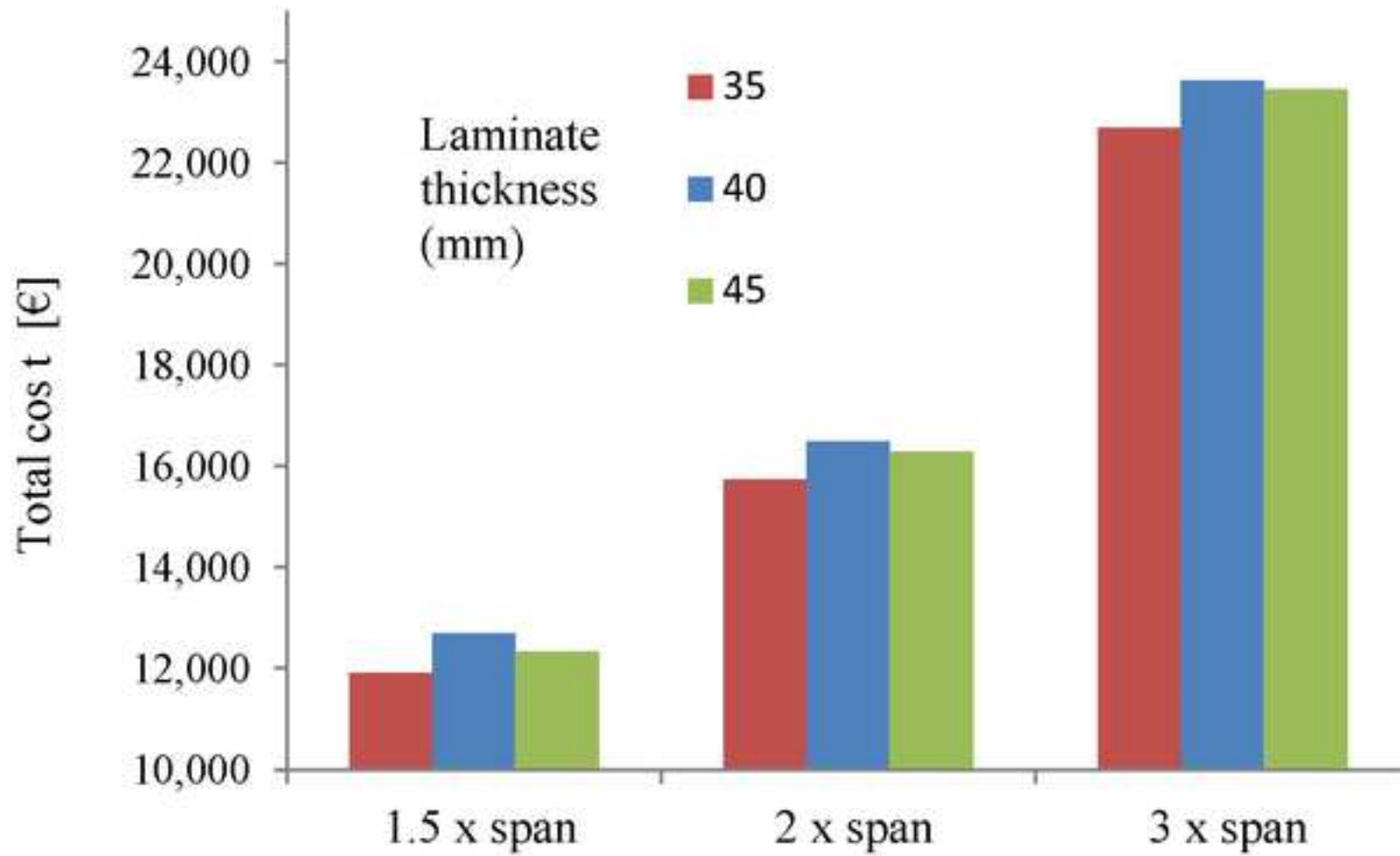


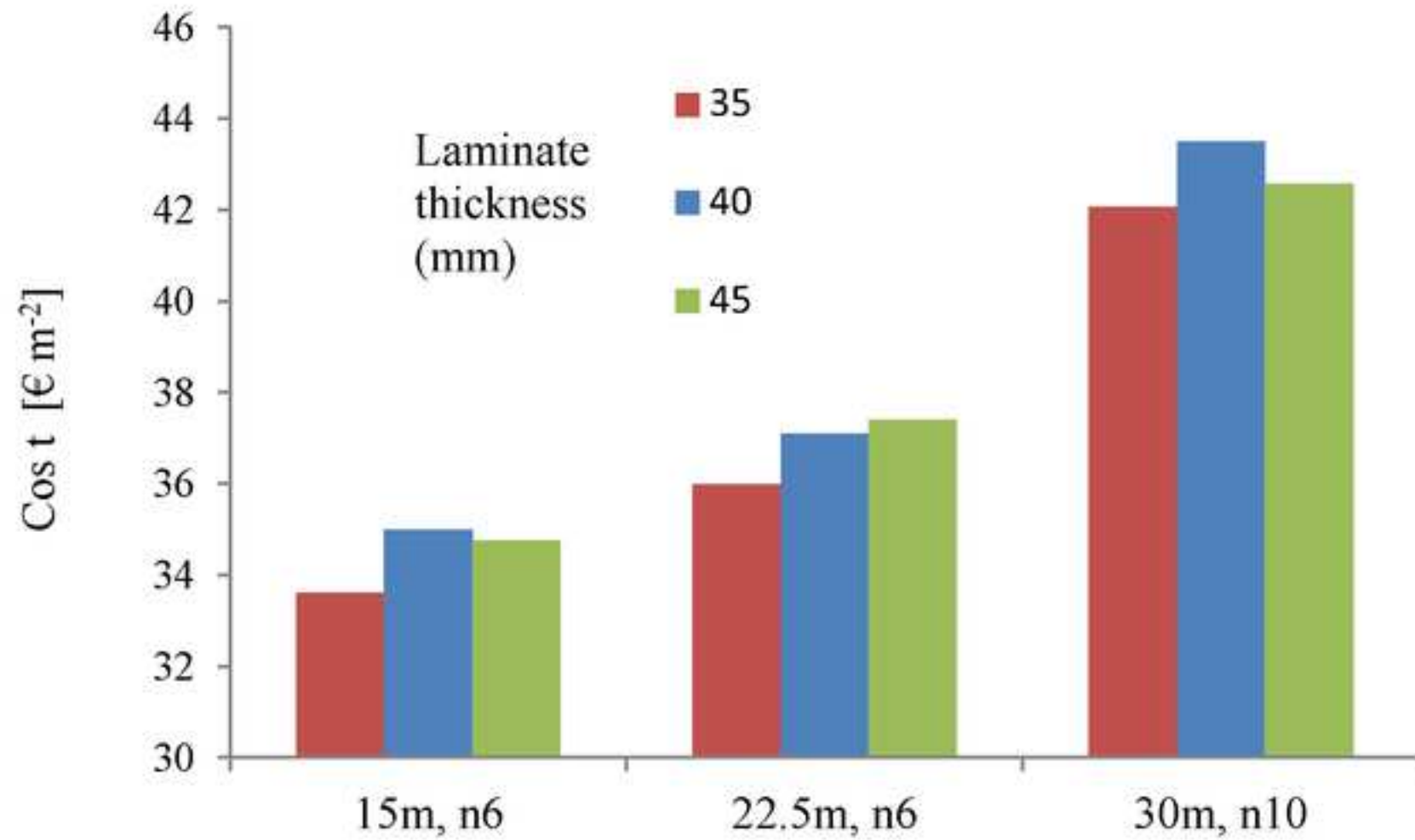














Click here to access/download

Table

Cost optimisation glulam timber roof
structures_ Tables.docx

